Diplomarbeit

Cellular biocompatibility on various dental materials

eingereicht von

Dr. med. univ. Stefan Heinrich Bubik

zur Erlangung des akademischen Grades

Doktor der Zahn-, Mund- und Kieferheilkunde

(Dr. med. dent.)

an der

Medizinischen Universität Graz

ausgeführt an der

Universitätsklinik für Orthopädie und orthopädische Chirurgie

In Kooperation mit der

Universitätsklinik für Zahnmedizin und Mundgesundheit / Klinische Abteilung für Zahnersatzkunde

unter der Anleitung von

Sen. Scientist Priv.-Doz. Mag. rer. nat. Dr. scient. med. Birgit Lohberger

Ao. Univ.-Prof. Dr. med. univ. Gerwin Arnetzl

Assoz.-Prof. Priv.-Doz. Dr. med. univ. Dr. med. dent. et scient. med. Michael Payer

Graz, 23.6.2016

Eidesstattliche Erklärung

Ich erkläre ehrenwörtlich, dass ich die vorliegende Arbeit selbstständig und ohne fremde Hilfe verfasst habe, andere als die angegebenen Quellen nicht verwendet habe und die den benutzten Quellen wörtlich oder inhaltlich entnommenen Stellen als solche kenntlich gemacht habe.

Graz, am 23.6.2016 *Dr. med. univ. Stefan Bubik e.h.*

Danksagungen

An dieser Stelle möchte ich all jenen meinen Dank aussprechen, die zur Entstehung der vorliegenden Diplomarbeit beigetragen haben.

Der größte Dank gebührt meinen Eltern ***Dr. med. univ. Michael Bubik*** und ***Karin Bubik***, die mich über die langen Jahre des Studiums begleitet und unterstützt haben. Ohne Ihre regelmäßige Motivation wäre dieser lange und beschwerliche Weg nicht bewältigbar gewesen.

Des Weiteren möchte ich mich bei meiner Betreuerin ***Priv.-Doz.in Dr.in Birgit Lohberger*** bedanken, die mir in jeder Phase meiner Labortätigkeit mit fachlichem Rat zur Seite gestanden hat. So manche Verständnisschwierigkeiten konnten durch Ihre Unterstützung schnell und effizient aus der Welt geschafft werden.

Insbesondere gilt mein Dank auch der praktischen Anleitung von ***Heike Kaltenegger, MSc*** und ***Nicole Stündl, BSc***. Ohne Ihre Hilfe und Erfahrung im Einsatz etablierter Methoden wäre dieses Projekt in diesem Zeitplan kaum zu realisieren gewesen.

Abschließend gilt diese Danksagung meinen beiden weiteren Betreuern ***Univ.-Prof. Dr. Gerwin Arnetzl*** und ***Assoz.-Prof. DDr. Michael Payer***, welche beide durch Ihre fachliche Exzellenz und ihre guten Kontakte zur Industrie unverzichtbare Anlaufstellen waren, wenn Fragen zu klinischen und materialtechnischen Aspekten dieser Arbeit auftauchten.

Inhaltsverzeichnis / Table of contents

Abkürzungen / Abbreviations

2D	Two-dimensional
3D	Three-dimensional
AB	Antibody
AB-dil	Antibody dilutent
ACTB	β-actin
Al_2O_3	Aluminum-trioxide (“Alumina”)
ASTM	American Society for Testing and Materials
ATCC	American Type Culture Collection
$BaSO_4$	Barium-sulfate
BIC	Bone-implant contact
BMP	Bone morphogenetic protein
BSA	Bovine serum albumin
C	Carbon
CAD/CAM	Computer-aided design/Computer-aided manufacturing
cDNA	complementary DNA
CFR	Carbon-fiber-reinforced
CM	Culture medium
CO_2	Carbon dioxide
cp-Ti	Commercially pure titanium
C_q	Quantification cycle
C_t	Threshold cycle
CT	Collection tube
Cy-2	Cyanine-2
DAPI	4',6-diamidino-2-phenylindole
DEPC	Diethylpyrocarbonate
DMEM	Dulbecco’s-modified Eagle’s medium
DNA	Deoxyribonucleic acid
EDTA	Ethylenediaminetetraacetic acid
EN	European norm
FBS	Fetal bovine serum
FDA	Food and Drug Administration
FEA	Finite Element Analysis
Fe	Iron

FeO	Iron-oxide
FGF	Fibroblast growth factor
g	G-force
GAPDH	Glyceraldehyde 3-phosphate dehydrogenase
GFR	Glass-fiber-reinforced
GPa	Giga Pascal
H	Hydrogen
HeLa	“Henrietta Lacks” immortal cells
hFOB	Human fetal osteoblasts
hGF	Human gingival fibroblasts
HPRT	Hypoxanthine phosphoribosyl-transferase
IF	Immunofluorescence
IgG	Immunoglobulin G
ILS	Internal Lane Standard
ISO	International Organization for Standardization
LDH	Lactate dehydrogenase
LSM	Laser scanning microscope
ME	Mercaptoethanol
MeSH	Medical Subject Headings
$MgCl_2$	Magnesium-chloride
MIQE	Minimum Information for Publication of Quantitative Real-Time PCR Experiments
MKI67	Marker of proliferation Ki-67
MM	Mounting medium
MPa	Mega Pascal
mRNA	Messenger RNA
MTS	3-(4,5-dimethylthiazol-2-yl)-5-(3-carboxymethoxyphenyl)-2-(4-sulfophenyl)-2H-tetrazolium salt
N	Nitrogen
NaO	Sodium-oxide
NAPDH/NADH	Nicotinamide adenine dinucleotide phosphate/ Nicotinamide adenine dinucleotide
NFW	Nuclease-free water

O	Oxygen
OD	Optical density
p	Passage
PAEK	Poly-Aryl-Ether-Ketone
PB	Protein Block
PBS	Phosphate-buffered saline
PCNA	Proliferating cell nuclear antigen
PEEK	Poly-Ether-Ether-Ketone
pFA	Para-formaldehyde
R_a	Mean surface roughness
RIN	RNA Integrity number
R_{mr}	Relative material ratio
RNA	Ribonucleic acid
rpm	Rounds per minute
RT-qPCR	Reverse transcription real-time quantitative polymerase chain reaction
R_z	Maximum roughness height
S_a	Arithmetic mean of the roughness of a surface area
SD	Standard deviation
S_{dr}	Density of peaks in a surface profile
SEM	Scanning electron microscopy
SiO_2	Silicium-dioxide
SLA	Sandblasted and acid-etched surface treatment
STR	Short tandem repeat
Ti	Titanium
Ti-6Al-4V	Titanium-6% Aluminum-4% Vanadium-Alloy
VCL	Vinculin
VIM	Vimentin
wt/vol	Weight per volume
XPS	X-ray photoelectron spectroscopy
Y_2O_3	Yttrium-trioxide (“Yttria”)
Y-TZP	Yttria-stabilized tetragonal zirconia polycrystal
ZrO_2	Zirconium-dioxide (“Zirconia”)

Abbildungsverzeichnis / Index of figures

Tabellenverzeichnis / Index of tables

Zusammenfassung

Einleitung: Der Ersatz verlorengegangener Körperanteile bleibt nach wie vor ein Hauptanliegen der medizinischen Forschung. Als Grundbestandteil bionischer Prothesen müssen sogenannte Biomaterialien eine Reihe an Tests durchlaufen, bevor sie als sicher genug für weitere biomedizinische Applikationen gelten. Einer dieser Tests ist die in-vitro Untersuchung in Zellkulturen. Die 3 Hauptgruppen an Biomaterialien in der Zahnersatzkunde sind Metalle, Keramik und Polymere. In der Implantologie gilt momentan reines Titan Grad 4 als Goldstandard. Zwei weitere Materialien, Zirkonoxid und Poly-Ether-Ether-Keton (PEEK), sind in den letzten Jahrzehnten zunehmend in den Mittelpunkt der implantologischen Forschung gerückt, da deren biomechanische und vor allem ästhetische Eigenschaften Vorzüge gegenüber Titan darstellen. Das Ziel dieser Studie war der Vergleich dieser 3 Materialien mit definierten Oberflächen und Zusammensetzungen unter gleichen Zellkulturbedingungen.

Methoden: Bredent Medical GmbH lieferte Scheibchen mit 14mm Durchmesser und 1mm Dicke gefertigt aus reinem Titan (cp-Ti), Yttrium-stabilisiertem Zirkonoxid (Y-TZP) oder gefülltem PEEK, welche spezifischen Oberflächenbehandlungen gemäß den firmeninternen Standards unterzogen wurden.

In der Zellkultur wurden humane fetale Osteoblasten (hFOB) und humane gingivale Fibroblasten (hGF) auf alle 3 Materialien ausgesät und nach 1, 3 und 7 Tagen auf Viabilität (MTS Assay) und Laktat-Dehydrogenase Ausschüttung (Cytotox Assay) untersucht. Zusätzlich wurden nach 3 Tagen die Proliferationsmarker PCNA und Ki67 (mRNA Expression), Änderungen der Zellmorphologie (Elektronenmikroskopie und Vimentin IF-Färbung), sowie Adhäsionsmarker (Vinculin IF-Färbung und mRNA Expression) bestimmt.

Ergebnisse: In hFOB Kulturen zeigte PEEK schlechtere Werte in Adhäsion und Viabilität im Vergleich zu den beiden anderen Materialien, welche ähnliche Werte wie die Kontrollgruppe aufwiesen. Die Zellen der hGF Kulturen lieferten vergleichbare Werte auf allen 3 Materialien, wobei auf PEEK eine minimal veränderte Morphologie in der Vinculin IF-Färbung sichtbar war.

Schlussfolgerung: Anhand der Ergebnisse dieser in vitro Untersuchung erscheint PEEK mit polierter Oberfläche aufgrund der schlechten Ergebnisse in hFOB Kulturen nicht ideal für die Anwendung als osseointegriertes Implantat. Für die Anwendung als prothetische Suprastruktur könnte es wegen der unveränderten Fibroblastenadhäsion aus biologischer Sicht durchaus als geeignete Alternative zu gängigen Materialien betrachtet werden.

Abstract

Introduction: Bionic replacement of deceased body parts remains a top priority in medical research. To approve the biocompatibility of the biomaterials applied in such devices, in vitro testing is one of the first in a sequence of steps necessary to render a material fit for medical application.

The three material groups used in dental prosthetics include metals, ceramics and polymers. The material of choice for dental implants is commercially pure titanium, while other materials such as zirconia and poly-ether-ether-ketone (PEEK) are considered highly promising due to their functional, biomechanical and esthetic properties.

The aim of this study was to determine whether PEEK with defined mean surface roughness and composition can retrieve results equal to machined titanium or zirconia.

Materials and Methods: Disks measuring 14mm in diameter and 1mm in thickness made from commercially pure titanium (cp-Ti), Yttria-stabilized zirconia (Y-TZP) and filled PEEK with specific surface finish were provided by Bredent Medical GmbH for cell culture experiments.

Human fetal osteoblasts (hFOB) and human gingival fibroblasts (hGF) were cultured on each material to observe changes after 1, 3 and 7 days in cell viability (MTS assay) and lactate dehydrogenase release (Cytotox assay). Additionally mRNA expression of proliferative factors PCNA and Ki67, cell morphology (Scanning electron microscopy and Vimentin IF-staining) and cell adhesion (Vinculin IF-staining and mRNA expression) was analyzed after 3 days in culture.

Results: In hFOB cultures, adhesion and viability was decreased on PEEK disks. No significant difference was observed in cp-Ti and Y-TZP when compared to control. In hGF cultures, all three materials performed almost equal, with only a slight difference in adhesion on PEEK disks in the Vinculin IF-staining.

Conclusion: Commercially pure titanium and Yttria-stabilized zirconia performed similar to control in all tests and remain two equal and reliable implant materials. It seems that highly polished PEEK in this particular composition cannot be recommended for osseointegrative applications such as dental implants due to decreased osteoblast attachment. Regarding fibroblast attachment to PEEK, usage in implant suprastructures such as abutments and dentures could be reasonable.

1 Introduction

„All right, listen. The Terminator's an infiltration unit: part man, part machine. Underneath, it's a hyperalloy combat chassis, microprocessor-controlled. Fully armored, very tough.
But outside, it's living human tissue: flesh, skin, hair, blood - grown for the cyborgs."
(Kyle Reese in "The Terminator") (1)

Although the term "bionics", defined as "the study of systems, particularly electronic systems, which function after the manner of, in a manner characteristic of, or resembling living systems", was first introduced to medical scientific literature in the early 1960s, according to the Medical Subject Headings (MeSH) database (2), the first documented approaches to artificial limb replacement and dental fixtures date back to the Egyptians and Etruscans (3,4). Back in ancient times, loose and fractured teeth were fixated using metal wires. Substitutes for lost fingers, arms and legs were fabricated as crude devices made from whole pieces of wood, leather and/ or metal. Limb replacement remained a privilege to the wealthy for centuries, only available to those who were able to afford the costs and lucky enough to endure the agony of amputation and to evade the then common complications of hemorrhage or severe wound infection. A famous example was the "knight with the iron hand" *Götz von Berlichingen*, who continued to fight with an iron replacement after his right hand was shot away in the battle of Landshut in 1505. *Ambroise Paré*, a surgeon in the French army in the 16th century, became famous for revolutionizing many methods in war surgery (including the ligation of blood vessels to prevent hemorrhage) and designing the first devices that were enabling its carrier to perform intricate articulating movements. In the following centuries improvements in anesthesia, surgery, material sciences and the understanding of biomechanics led to a vast amount of possibilities in treatment of limb loss and, generally speaking, defects in the integrity of the human body. (3)
In addition, it became important to make a distinction between bionic devices that are self-retaining and in superficial/external contact with the body and those mounted internally to the human musculoskeletal system and in direct contact with living cells of the body's inner tissues, so-called "implants".

Also referred to as Prosthetics (derived from the Ancient Greek word *prósthesis*, meaning “addition”, “application” or “attachment”), these devices are able to match the missing body parts in function, size, weight, shape and color, even enabling formerly disabled individuals to perform in high-intensity competitions such as the Olympic Games and setting records similar to those of their non-disabled colleagues.(5)

In Prosthetic Dentistry, high-intensity competition remains limited to the acts of mastication, phonation and social interaction. On first sight, advances in prosthodontic technology may not seem as obvious to the external spectator as the ones in the Orthopedic field, but to those suffering from tooth loss, particularly in the posterior regions of the dental arch, the current state-of-the-art therapy with implant-supported dentures has brought major improvements in quality of life compared to traditional treatment with partial or complete mucosa-borne dentures. As the mean age in western society and therefore the number of patients suffering from partial or total edentulism is on the rise, such issues have gained further importance. It seems that complete denture wearers restrict and alter their diet due to development of significant functional impairments in the long-term, especially with progressive alveolar atrophy of the mandible. Apart from a decrease in the overall nutritional status of the patient, the resulting change of diet can contribute to an increased rate of intraoral swelling and/or pain. A growing number of studies suggest that complete denture wearers with reduced masticatory efficiency suffer not only from nutritional restrictions but are also prone to social constraints. (6)

1.1 Biomaterials in Medicine

A crucial aspect of advances in every technological field is the constant improvement of existing and applied technologies. Thus it is necessary not only to develop an evolving understanding of function (in our case the understanding of a bionic replacement) but also to question the application of currently used components. In medicine, these components are referred to as *biomaterials*, which are defined as “substances that have been engineered to take a form which, alone or as part of a complex system, are used to direct, by control of interactions with components of living systems, the course of any therapeutic or diagnostic procedure, in human or veterinary medicine” (7). This definition might sound a little vague at first, but considering the vast diversity of materials tested in the medical

literature in the last 10 years alone, it is perfectly reasonable. Entering the word "biomaterials" into PubMed with a limit on the last 10 years, one yields approx. 10.000 results compared to 4.100 results in all the years before 2006.
Tissue tolerance is accounted for through the concept of *biocompatibility*:
"Biocompatibility refers to the ability of a biomaterial to perform its desired function with respect to a medical therapy, without eliciting any undesirable local or systemic effects in the recipient or beneficiary of that therapy, but generating the most appropriate beneficial cellular or tissue response in that specific situation, and optimizing the clinically relevant performance of that therapy." (8)
Whether a host-response in terms of a Host vs. Graft reaction is taking place, depends on multiple factors (Table 1).

Bulk material composition, micro- (or nano)-structure, morphology
Crystallinity and crystallography
Elastic constants
Water content, hydrophobic–hydrophilic balance
Macro-, micro-, nano-porosity
Surface chemical composition, chemical gradients, surface molecular mobility
Surface topography
Surface energy
Surface electrical/electronic properties
Corrosion parameters, ion release profile, metal ion toxicity (for metallic materials)
Degradation profile, degradation product form and toxicity (for polymeric materials)
Leachables, additives, catalysts, contaminants and their toxicity (for polymeric materials)
Dissolution/degradation profile, degradation product toxicity (for ceramic materials)
Wear debris release profile

Table 1: Major material variables that may influence the host response. (adapted from Williams DF) (8)

The basis of modern biomaterials is still one of three substances: metals, ceramics and synthetic or biological polymers. The biggest changes however occurred in the methods of fabrication and the way in which materials are combined into composites to complement each others' advantages and outweigh disadvantages. While in the past a bionic implant was usually made of one structural biomaterial constructed to avoid direct host interaction (so-called bioinert materials that were meant to be invulnerable to chemical and physical wear) and achieve a maximum of stability, modern materials try to mimic the desired tissue in relation to primary

stability, tensile strength, fracture resistance, degradation and overall appearance. The traditional concept of bioinert materials feels more and more inapplicable as degradation processes such as age-dependent down wearing and corrosion became known throughout the years with even the most trusted material. The term *bioactive* is trying to address these issues in a way that materials are being constructed to interact with the complex configuration of the material-tissue interface and biodegradation is being taken into account as a part of the integration process into the living system (9). Both surface modification (on the 2D-level) and the fabrication of porous materials (on the 3D-level) are methods to address these ideas.

Various production methods have been applied since the dawn of (bio-) material sciences, including casting, molding, polymerization, deep-freezing, electrospinning etc. The primary methods of choice for industrial production of prosthetic materials are casting, firing and injection molding.

In essence, once the single components of a metal/ceramic/polymer are identified and purified, they are usually combined and casted either into a final shape (dental implants, joint prosthetics, etc.) or a solid block of the desired composition that can be further customized through machining. The most advanced machining technique applied in dentistry is the CAD/CAM method (short for Computer Aided Design/Computer Aided Machining). A fired/polymerized solitary block of ceramics or a ceramic-enhanced polymer is being modified with mounted burrs in an automated process. A commonly used system is Sirona's CEREC® product line (10) (Fig. 1).

Figure 1: The CEREC® MC and AC machining and designing units. (Printed with permission from Sirona Dental Systems Gmbh, Bensheim, Germany) (10)

1.2 Dental implant materials

The dental implant is the bionic replacement of the single tooth or, more precisely, its root. In the common two-piece system, the construction includes the screw-shaped implant and its suprastructure, the so-called abutment (Fig. 2).

When back in the 1960s Per-Ingvar Brånemark discovered that imminent contact of pure titanium (Ti) implants with living bone results in the "direct structural and functional connection between living bone and the surface of a load-bearing artificial implant"(11), a process he later coined "Osseointegration", the dental discipline of *Implantology* was born.

Figure 2: A common two-piece implant system consisting of the implant and abutment.

In short, the process is similar to fracture healing with the small difference of the lack of a chondrogenic precursor (or "callus"). After roughly 12 - 16 weeks, the process should be completed. "Direct connection" in this case refers to the condition where bone tissue is adapting to the implant's surface without the formation of any reactive fibrous tissue, influencing the long-term stability of the procedure. Histologically speaking, only a single layer of fibers is formed which, in thickness and consistency, resemble the Sharpey's fibers of the natural tooth, also acting as a biological seal against microbiological infiltration. A histological difference is only made in the orientation of the filaments that, instead of approaching the surface perpendicularly as observed in the natural tooth, now run parallel to the implant's surface.

In 1981, Albrektsson and Brånemark defined six factors for successful incorporation of the implant (12):

1. Biocompatibility of the implant material
2. Macroscopic and microscopic nature of the implant surface and designs
3. The status of the implant bed in both a health and a morphologic (bone quality) context
4. The surgical technique per se
5. The undisturbed healing phase
6. Loading conditions

Surface roughness has been described as a major factor in inducing bone formation on the implant's surface and has been divided into 4 categories depending on the S_a value (representing the arithmetic mean of the roughness of a surface area from the mean plane): smooth (S_a < 0.5 µm); minimally rough (S_a between 0.5-1.0 µm), moderately rough (S_a between 1.0-2.0 µm) and rough (S_a > 2.0 µm). (13)
A number of studies in animals have shown that moderately rough surfaces with an S_a of about 1.5 µm and an S_{dr} value (the density of peaks in a surface profile, representing the relative surface enlargement) of 50% strongly improve the bone's reaction. (14)
The type of material used also needs to be considered as its hardness directly influences the roughness obtained with the treatment. The same treatment will yield a different surface roughness in different materials. (13)

Even though it has been produced in its modern composition by the metal industries since the early 1940s and constantly been applied in aircraft and spaceship construction, it was not until the 1980s and the establishment of osseointegration that commercially pure titanium (cp-Ti) quickly became the biomaterial of choice for a wide range of medical indications, including joint replacement in Orthopedic Surgery and the treatment of cranial defects in Oral- and Maxillofacial Surgery/Neurosurgery, due to its highly favorable strength to weight ratio, biocompatibility and resistance to corrosion.
The initial formation of a passive oxide-layer on cp-Ti seems to be the main reason for its high stability in fluids at physiological pH-values and its low corrosion current. (15)
Titanium and its alloys are classified into Grades 1-38 depending on their chemical purity and according to the *American Society for Testing and Materials'* (ASTM) Standards (16). Pure titanium is categorized into Grades 1-4, while its alloys are graded Grade 5 and above, starting with Ti-6Al-4V, the most fabricated titanium product in the metal industries.
While Grade 4 titanium is strong enough for the dental implant body itself, its yield strength of roughly 200 Mega Pascal (MPa) can barely deliver enough fracture resistance to small spare parts such as screws and suprastructures. Further strength is gained through alloying Ti with 6% aluminum and 4% vanadium (Ti-6Al-4V), partially inhibiting the conversion of high-temperature β-phase Ti into low-

temperature α-phase Ti, thus raising the yield strength of this alloy to roughly double the value (~400 MPa) of cp-Ti. (17)

Even though higher strength means higher fracture resistance of the Implant material, titanium's elasticity (Young's) modulus of approximately 104 Giga Pascal (GPa) appears to be too high compared to bone's elasticity modulus of 10-30 GPa which can be inhibiting to bone remodeling (15). Surface and structural modifications (including research in new types of alloys) are possible ways to address this issue.

Another point of critique is the rising worry about allergies to titanium. A study on 1500 patients exposed to cp-Ti-Implants determined an allergy prevalence of 0.6% (18).

In addition, deposition of oxidative metal ions in adjacent tissues released from titanium has been reported in in-vitro experiments, but its clinical implication has not been proven yet (19).

Under certain conditions (e.g. in the case of a thin gingival biotype of the marginal gingiva), the gray color of Ti-based Implants and abutments can lead to undesirable esthetic downturns (Fig. 4) (20).

Figure 3: Visible titanium post after recession of the marginal gingiva. (adopted from Mellinghoff 2014) (20)

Ceramic materials seem to be a promising solution to these issues.

Tooth-like color, low plaque affinity and high corrosion resistance have already made them popular materials for the application in restorative dentistry and orthodontics. It is known though that ceramics are susceptible to shear and tensile stress. Flaws on the surface can lead to failure or, in other words, imply a certain risk of fracture. (21)

Ever since Ti-based Implants were introduced clinically 30 years ago, Aluminum (Al_2O_3)-based ceramics were tested for Implant purposes but were found to lack resistance to fracture in the long-term use.

The much tougher material zirconia (ZrO_2) received good reputation in the last decades due to its unique mechanism of *transformation toughening*: Through addition of a small percentage of 3-5 Mol-% of Yttria (Y_2O_3), heated ZrO_2 remains in its polycrystalline tetragonal state either fully or partially when cooled down to room temperature (Fig.3) (22). Whenever a crack in the material occurs, immediate conversion of tetragonal into monoclinic zirconia is taking place in the fracture site, a process which goes along with an increase of volume that prevents the progression of the crack.

As a result, high flexural strength (900–1.200 MPa), Vickers' hardness (1.200), elasticity (Young's) modulus (210 GPa) and Weibull modulus (10–12) occur in Yttria-stabilized tetragonal zirconia polycrystal (Y-TZP). (21)

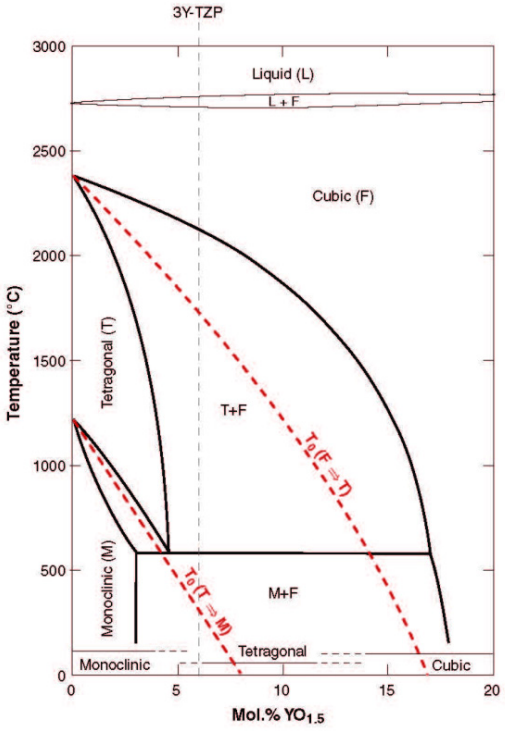

Figure 4: ZrO2–YO1.5 phase diagram. Metastable phases retained at room temperature are indicated just above the horizontal axis. The red dotted lines show the nonequilibrium monoclinic-tetragonal and cubic-tetragonal transition regions. (adopted from Chevalier et al. 2007) (22)

Several animal experiments in monkeys and dogs showed comparable results of surface-modified zirconia implants compared to commercially available cp-Ti implants. Both removal torque and bone-implant contact (BIC) were reported to be similar. (23)

Limitations to the use of zirconia-based ceramics (especially of Y-TZP) in implants and suprastructures include low-temperature degradation in the wet environment, low bonding strength due to its acid-resistant properties and therefore higher rates of fractures, delamination and chipping compared to porcelain fused-to-metal restorations. (24)

Currently, most commercially available zirconia implants are designed as single-piece implants (combined implant body and abutment), which means these implants have to be modified intraorally through grinding on their supracrestal structure to fit the restoration. This lack of prosthetic versatility leads to

compromised implant positioning, especially if angulated supracrestal structures are needed in areas such as the esthetic zone.

Also, sufficient clinical long-term data is limited for zirconia-based implants. (25)

Only recently a prospective randomized-controlled trial by Payer et al. has presented promising results with two-piece zirconia implants with no clinical difference when compared to titanium two-piece implants in a 24-months observation. (26)

As mentioned above, the use of materials with a significant mismatch of the elasticity (Young's) modulus when compared to bone can result in even higher stress peaks at the bone-implant interface and could negatively influence bone remodeling.

Polymers are able to match bone's mechanical properties and are already being widely used in other surgical fields such as Orthopedics, Traumatology and Neurosurgery for the bionic replacement of calvarial and spinal defects.

Among the extensive field of polymer sciences, the group of Poly-Aryl-Ether-Ketone (PAEK) and its derivate Poly-Ether-Ether-Ketone (PEEK) have shown the most promising results when it comes to mechanical strength, stiffness, structure, thermal and chemical resistance. PEEK is a thermoplastic polymer that is generally colorless, making it a suitable material for dental application in the highly esthetical regions. Its biocompatibility seems to be as high as in other widely used biomaterials, referring to almost 30 years of clinical evidence. Even though unfilled polymers of the poly-aromatic type exhibit an elasticity (Young's) modulus of 3-4 GPa, the elasticity modulus can be adapted to match bone (1-15 GPa) or even titanium alloy (110 GPa) through fabrication of carbon-fiber-reinforced (CFR) or glass-fiber-reinforced (GFR) composites with variable fiber length and orientation.(27)

Current dental applications include restorative implant suprastructures such as overdenture-bars. The use of PEEK as an osseointegrated implant material is limited yet by its bioinert property and low cell adhesion rate in the unmodified state. Another issue is the susceptibility of polymers to moisture expansion and consequent attachment and infiltration by microorganisms. Additionally, if the material's elasticity modulus is too low, high load concentration does occur at the cortical bone of the cervical margin in the implant site. (28)

In a Finite Element Analysis (FEA) conducted by Schwitalla et al., CFR-PEEK with 60% of endless carbon fibers appears to have similar mechanical qualities and stress distribution at the bone-implant interface when compared to titanium. (29)

As CFR-PEEK is gray due to the added carbon fibers, positive mechanical properties are outweighed by its appearance, making it unfavorable for critical esthetic indications (Fig. 5) (30).

With only 2 in-vivo animal studies demonstrating mixed results and no long-term clinical experience available in the application as dental implants, PEEK remains far from being recommendable for clinical use in Implantology. (28)

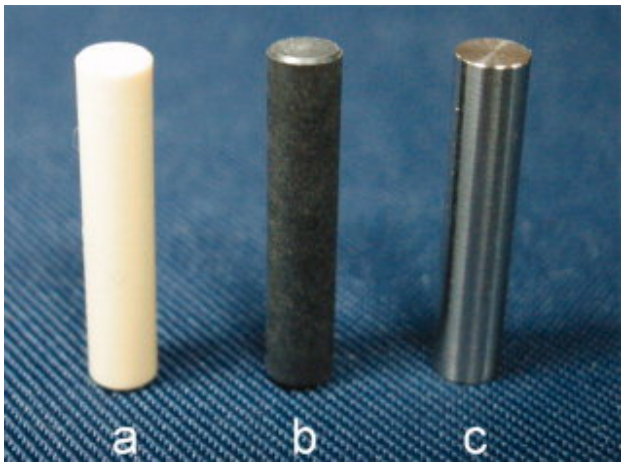

Figure 5: **a: glass-fiber reinforced PEEK;**
b: carbon-fiber reinforced PEEK;
c: titanium rod
(adopted from Lee et al. 2012) (30)

Sisomm, an Implant manufacturer from Belgium, is already offering single-piece PEEK implants (called PERSO® implants made from PEEK OPTIMA® with 6% Bariumsulfate for increased radio opacity) in three sizes with differing diameter and length.

Another model, the BIOPIK® single-piece implant made by IMI of France, comes in three designs and is made from PEEK OPTIMA® filled with titanium or tricalciumphosphate, but lacks the feature of radio opacity. (31)

1.3 Biocompatibility Testing

To ensure safety of an implanted biomaterial, a strict routine has been implemented since the 1980s to meet the growing demand for standardized pre-clinical testing (8).

A new material must be cleared by the American Food and Drug Administration (FDA) before being rendered safe for medical use. Modern protocols are based on the EN ISO 10993 “Biological Evaluation of Medical devices” standard tests 1-20.(32)

These protocols include physical, chemical as well as biological in-vitro and in-vivo examinations for acute/chronic and local/systemic effects of the designated biomaterial on mammalian tissue.

Common protocols for attesting biological safety include tests for:

-Cytotoxicity

-Sensitization

-Hemocompatibility

-Pyrogenicity

-Implantation

-Genotoxicity

-Carcinogenicity

-Reproductive and Developmental Toxicity

-Biodegradation Testing

For in-vitro testing, cells are being chosen that are similar or closely match the cells in immediate contact with a device at the future site of implantation.

In the case of dental implants, such cells would be either of osteogenic or fibrogenic origin, predominantly osteoblasts and fibroblasts.

Out of the three functional cell types in bone's original tissue (namely osteoblasts, osteocytes and osteoclasts) osteoblasts retain the function to proliferate and rebuild lost bone tissue through excretion of bone matrix and its calcification. They originate in the stromal cells of the bone marrow and the bone's surface (including the perivascular regions) and differentiate into osteocytes. (33)

Fibroblasts are responsible for the regeneration of connective tissue's extracellular matrix and differentiation into fibrocytes, its predominant structural cell. Their potential to differentiate into any kind of mature mesenchymal tissue is widely known.

For the above mentioned materials (cp-Ti, Ti-6Al-4V, Y-TZP and unfilled PEEK), a variety of in-vitro and in-vivo tests has been performed over the last decades that qualify them for the application in medical devices. (15,23,27)

1.4 Aims of this study

Three implant materials with defined surface properties (cp-Ti, (Y-)TZP-A, filled PEEK) are being tested on their short-term effect on osteoblast and fibroblast viability, cytotoxicity, histomorphometry of adhesion and gene patterns of proliferation in comparison to standard cell laboratory culture plates.

Even though many in-vitro studies have shown the biocompatibility and osseointegrative features of each single one of these materials, no study has yet tried to apply standardized comparable conditions under which all three materials are being tested simultaneously.

In respect to future developments in polymer affiliated implant and dental restorative materials based on PEEK, the question to be solved is the following:

Is the highly customable, lightweight, tooth-like colored and metal-free material PEEK able to match up to the already well-known and clinically tested materials when it comes to biocompatibility and the facilitation of cell proliferation?

2 Materials and Methods

2.1 Tested biomaterials

Three materials were tested: commercially pure titanium Grade 4 (cp-Ti), Yttria-tetragonal-Zirconia-polycrystal ((Y-) TZP-A) and poly-ether-ether-ketone (PEEK) filled with ceramic particles sized 0.3-0.4 µm (see table 2 for composition in vol%).

Cp-Ti	~99% Ti	<0.50% Fe	<0.40% O	<0.08% C	<0.05% N	<0.0125% H
(Y-)TZP-A	94.5±0.5% ZrO_2 (+HfO_2)	5.2±0.1% Y_2O_3	0.25±0.05% Al_2O_3	<0.5% SiO_2, FeO, NaO		
Filled PEEK	77±3% PEEK	3±3% $BaSO_4$	19±3% Al_2O_3, ZrO_2, TiO_2	<2% pigments (e.g. FeO)		

Table 2: Material composition in their final state (parameters provided by Bredent Medical GmbH).

The tested materials were manufactured and modified by Bredent Medical GmbH (Senden, Germany) as follows:

All three materials were molded into rods, cut and burred into disks measuring 14mm in diameter and 1mm in thickness to fit the 24-well plates applied in cell culture experiments. Surface treatment was conducted according to the manufacturer's standards through machining (detailed procedure not disclosed).

After surface modification, surface finish roughness was measured by optical profilometry in a two-dimensional (2D) plane (either horizontally or vertically) according to the ISO 4287 standard.

The amplitude parameters maximum roughness height (R_z; mean of highest peaks and lowest valleys in five separate sample lengths) and mean surface roughness (R_a; arithmetic average of absolute roughness values, displaying the deviation from the arithmetic mean line of all peaks and valleys within a sample length) as well as the material parameter of relative material ratio (R_{mr}; relative material ratio

of the roughness profile, displaying the consistency of the surface profile) were calculated from the roughness profile (34). Only the data of PEEK disks was provided by the manufacturer (refer to Table 3).

	Number of measurements (n)	Ra (µm)	Rz (µm)	Rmr (%)
Horizontal	3	0.018±0.0007	0.137±0.01	100%
Vertical	3	0.018±0.002	0.142±0.02	100%

Table 3: Roughness parameters after surface finish on PEEK samples. R_a and R_z values are displayed as mean ± SD. (data provided by Bredent Medical GmbH, measurement conducted by Dr. M. Schmid)

Prior to usage, the platelets were placed in an ultrasound cleansing device for approximately 30 minutes, dabbed dry with clean paper towels, packaged in autoclavation bags and consecutively sterilized in a steam pressure tabletop sterilization chamber (GetingeK5+, Getinge Vertrieb und Service GmbH, Rastatt, Germany) for approximately 30 min at 134°C.

2.2 Cell culture

Human fetal osteoblast cells (hFOB 1.19; ATCC® number: CRL-11372™; LGC Standards, Middlesex, UK) were cultured in Dulbecco's-modified Eagle's medium without phenol red (DMEM-F12; GIBCO® Invitrogen, Darmstadt, Germany), containing 10 % fetal bovine serum (FBS), 1 % L-Glutamine, 100 units/ml Penicillin, 100 µg/ml Streptomycin, 0.3 mg/ml Geneticin G418 (all GIBCO® Invitrogen) and 0.25 µg Amphotericin B (PAA Laboratory, Pasching, Austria). For expansion cells were incubated at 34°C in a humidified atmosphere of 5 % CO_2, and medium was subsequently replaced every 3-4 days until cell density reached a confluence of approximately 90%.

Human gingival fibroblasts (hGF; Cell Lines Service, Eppelheim, Germany) were cultured in fibroblast basal medium containing supplement mix (PromoCell, Heidelberg, Germany), 100 units/ml Penicillin, 100 µg/ml Streptomycin (all GIBCO® Invitrogen) and 0.25 µg Amphotericin B (PAA Laboratory). For expansion cells were incubated at 37°C in a humidified atmosphere of 5 % CO_2, and medium

was subsequently replaced every 3-4 days until cell density reached a confluence of approximately 90%.
All cell lines were verified by short tandem repeat analysis using the Power Plex 16® System Kit (Promega, Mannheim, Germany):
3.5x 10^4 cells from either hFOB or hGF were resuspended in 200 µl PBS and mixed with 20 µl Proteinase K and 200 µl AL Buffer (Qiagen). DNA preparation and normalization was accomplished using the QIAamp DNA Mini kit (Qiagen) according to the manufacturer's protocol. Subsequently, 1 µl of each sample was amplified applying the Power Plex® 16 System (Promega) in a 10µl reaction. 1 µl of the product was mixed with Hi-Di formamide and Internal Lane Standard (ILS 600, both: Applied Biosystems Inc., Foster City, CA), denatured and fractionated in the ABI 3730 Genetic Analyzer (Applied Biosystems Inc.). Data was processed and evaluated using ABI Genemapper 4.0 (Applied Biosystems Inc.).

For subculture or experimental manipulations adherent cells were washed with PBS 1x, containing phosphate-buffered saline pH 7.2 - 7.3 (PAA Laboratory), 100 units/mL Penicillin, 100 µg/mL Streptomycin (all GIBCO® Invitrogen) and 0.25 µg Amphotericin B (PAA Laboratory),and detached with the appropriate amount of Accutase™ (Sigma Aldrich, St.Louis, MO) for 5 minutes at 34°C or 37°C. After resuspending the detached cells with the particular culture medium, the suspension was centrifuged at 300x g for 7 min. The pellet was resuspended with 10 ml of culture medium and the number of viable cells was determined with a hemocytometer: 20µl of cell suspension were mixed with the equal volume of trypan blue (Sigma Aldrich), the cell number was calculated and the cells were seeded for expansion or experimental manipulations.

Subsequently, cell lines determined for experimental manipulations were seeded on cp-Ti, PEEK, or Y-TZP platelets placed in 24-well Corning® Costar® Ultra-Low attachment multiwell plates (Corning Inc., Corning, NY) and control cells were seeded on conventional tissue culture-treated 24-well plates made from polystyrene (TPP, Trasadingen, Switzerland) according to our schematics (Fig. 6).

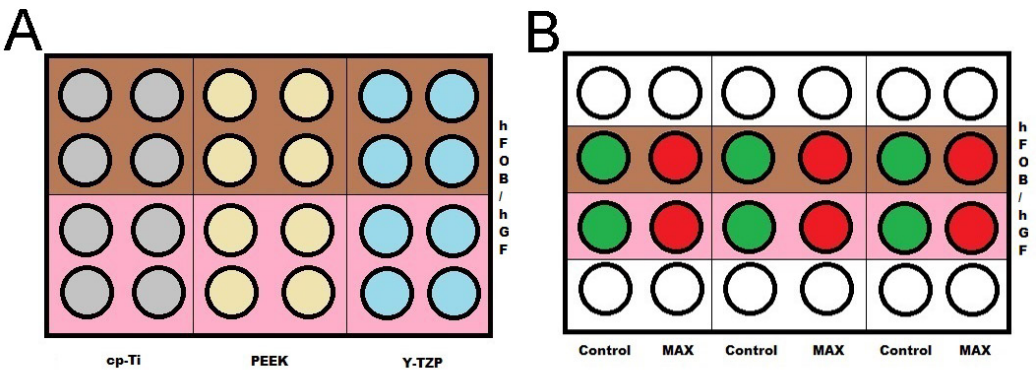

Figure 6: Seeding schematics for cell culture experiments; Cells were seeded into each well of A) 24-well Low Attachment plates pre-assembled with material disks and B) additionally for MTS and Cytotox assays' control and maximum LDH release (MAX) into polystyrene control plates.

2.3 Cell viability assay

Often referred to as the MTS/MTT-assay, this procedure is based on a tetrazolium salt compound, the so-called Owen's reagent, and an electron coupling reagent. The whole enzymatic reaction is catalyzed by the NADPH/NADH system inside the cell. When added to the cell culture, the solution is metabolized by living cells into a colored formazan product that can be measured in a common spectrophotometer at absorbance values of 490/650nm. After deduction of the background values (usually culture medium alone), the results correlate directly with the number of living/metabolically active cells. (34)

1.5x 10^4 cells/cell-type were seeded in each well. After one, three and seven days of culture the CellTiter 96®AQ_{ueous} One Solution Cell Proliferation Assay (Promega) was performed in accordance with the manufacturer's instructions. The culture medium was used as a background measurement. Absorbance values were measured in the Spectrostar™ spectrophotometer (BMC Labtech, Ortenberg, Germany).

Detailed protocol for MTS measurement:

Things to consider:

- ☐ Resuspend the cell suspension before counting for most reliable results
- ☐ MTS assay is photosensitive and should be pipetted and incubated under minimum lighting for best results

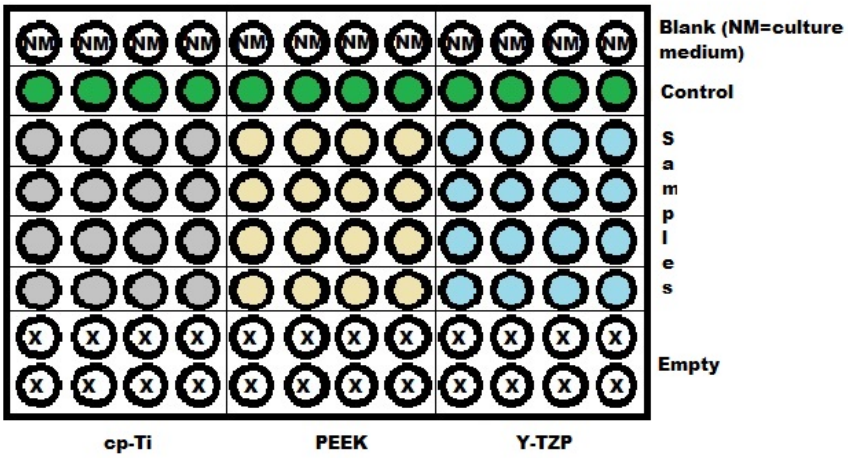

Figure 7: Schematics for 96-well plate in MTS-measurement.

Procedure:

- Label the 96-well plates (refer to Fig. 7 for schematics)
- Prepare the culture medium-MTS mixture for one well by adding 100 µl CellTiter 96®AQ_{ueous} One solution to 600 µl of culture medium (CM) or for 36 wells by adding 3,6 ml CellTiter 96®AQ_{ueous} One solution to 21,6 ml of CM, respectively
- Discard the supernatant from each well of the 24-well plates (samples and control), add 600µl of CM-MTS mix instantly into each well to avoid excess drying and cell-death
- Incubate the sample and control 24-well plates and the remaining CM-MTS mix for 2-3 hours at 34°C or 37°C in a humidified atmosphere of 5 % CO_2.
- After 2-3 hours (depending on the color switch in the MTS wells), pipette 100µl of CM-MTS mix/well into the Blank-wells on the regular 96-well plates
- Pipette 4x 100µl of each sample and control well into the 96-well plate according to the schematic (avoid bubbles!)
- Instantly proceed to spectrometric measurement

2.4 Cytoxicity assay

Lactate dehydrogenase (LDH) activity was determined using the CytoTox-ONE™ Homogeneous Membrane Integrity Assay (Promega). In the living organism, LDH is usually present inside the living cell only, with high amounts of LDH occurring solely in areas of cellular damage where the enzyme is released into the neighboring tissue. The amount of fluorescence measured is therefore proportional to the percentage of damaged cells in a culture. (35)

1.5x 10^4 cells/cell-type were seeded in each well. After one, three and seven days of culture, cell culture supernatants were processed and analyzed according to the manufacturer's protocol. Fluorescence was measured at 560/590 nm in the Fluostar™ system (BMC Labtech).

Detailed protocol for Cytotox measurement:

Things to consider:

- ☐ The Cytotox-solution is highly susceptible to light – work under minimal lighting conditions and cover the plates at all times in alumina foil when they're not being worked with!

Prepare the following:

- ☐ Prepare Cytotox one Reagent by adding 11ml of Assay Buffer to one vial of substrate. Mix gently to solve the substrate

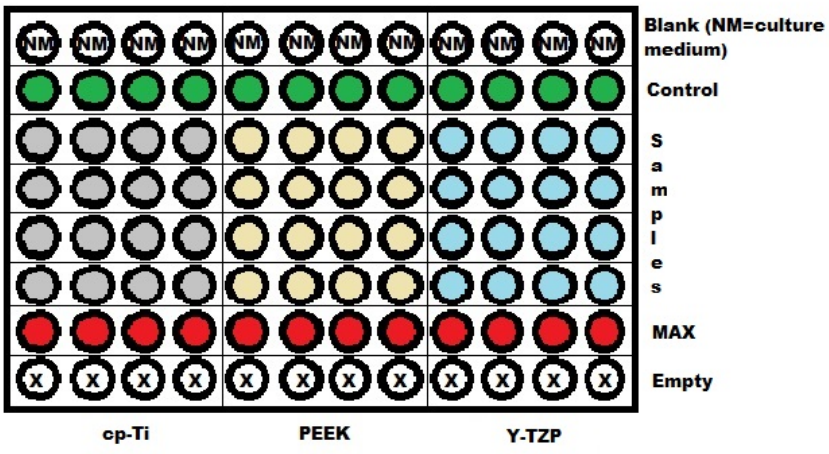

Figure 8: Schematics for 96-well plate in Cytotox-measurement.

Procedure:

- Label the 96-well plates (refer to Fig. 8 for schematics)
- Pipette 4x 50µl of cell culture supernatant from each well of the 24-well plates (samples or control) into a white 96-well plate (refer to schematic)
- Pipette 50µl of CM into the Blank-wells on the white 96-well plate
- Cover the white 96-well plates with alumina foil
- Add 20µl of Lysis buffer (2µl/100µl) to the „MAX“-wells on the 24-well plate and incubate for 10 min
- Pipette 4x 50µl of the MAX-wells into the white 96-well plates (see schematic)
- Add 50µl of Cytotox reagent to all wells on the white 96-well plates and incubate for 10 min at room temperature, light protected
- Add 25µl of the stop solution to each well, mix through shaking the plate lightly, cover the plate in alumina foil and proceed instantly to fluorescence measurement on the Fluostar™ device

2.5 RT-qPCR analysis

Reverse transcription real-time quantitative polymerase chain reaction (RT-qPCR) represents one of several variations of the commonly used quantitative PCR methods to measure ribonucleic acid (RNA) expression patterns (the essential steps of this procedure are shown in Fig. 6) (36). As described in the 2009 published Minimum Information for Publication of Quantitative Real-Time PCR Experiments (MIQE) guidelines, certain requirements should be met to ensure the quality of the laboratory procedure (37).

Essentially, RNA from living cells in animal or plant cell cultures or tissues is extracted by enzymatic lysation and purified through several washing steps to remove any genomic nucleic residues. In addition, quantity and quality of the RNA samples should be controlled in a separate step. (37)

The sample is marked with a non-specific genetic "primer" sequence, a short nucleic acid sequence that is able to bind to certain complementary regions on a genetic nucleic acid strand and act as a starting point for deoxyribonucleic acid (DNA) synthesis or amplification. The hybridized RNA strand is then converted into complementary DNA (cDNA) using the enzyme reverse-transcriptase, an enzyme discovered in the viral replication of genomic sequences. The whole reaction takes place in a thermocycler, a device routinely applied in molecular biology to catalyze enzymatic reactions through temperature regulation.

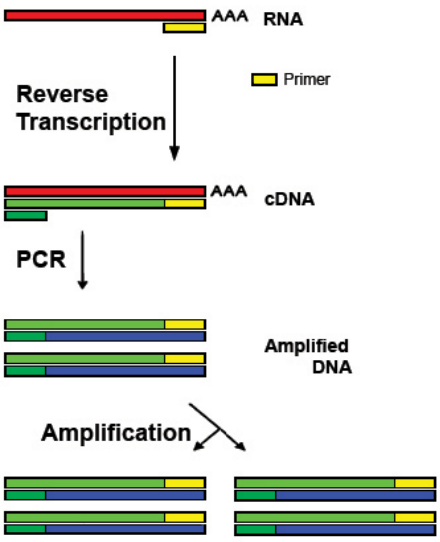

Figure 9: The essential steps of RT-qPCR. (adopted from Wikipedia) (36)

Consecutively, cDNA is purified through washing before the sample is being prepared for the qPCR:

First, a specific primer is added to mark the desired target sequence (the so-called amplicon) on the cDNA strand. To ensure the stability of the sample and to be able to calibrate the results, primers for certain ubiquitous cellular reference genes (sometimes referred to as housekeeping genes) should also be included in the analysis.

Second, the so-called mastermix, a mixture of a DNA-polymerase, deoxyribonucleotides and buffer solution, is added to the sample to provide the essential substrates for DNA-polymerization and amplification.
Third, a DNA-binding substance marked with a fluorphore (a fluorescent chemical compound) facilitates the detection and quantification of DNA amplification (or non-amplification) in real-time at a certain stage of each PCR cycle. Fluorescent markers can be either specific or non-specific to certain DNA sequences. A traditional example for a non-specific marker would be ethidium bromide, nowadays replaced by safer agents such as SYBR® Green I dye.
In a common PCR cycle, the sample is again placed in a thermocycler after adding the above mentioned reagents and heated to 95-98°C to separate the DNA strands, then cooled down to 50-60°C for the binding of the primers, and finally heated again to approximately 70°C for the polymerization process.
Fluorescence measurement is conducted at the end of each cycle, with the total number of cycles usually varying between 25-50 cycles.
Results of the analysis are shown in fusion temperature/melting curves, where the melting temperature is specific to the amplified gene. For quantification purposes, a threshold is defined through background fluorescence measurement that needs to be exceeded by the measured sample 3-5 times the signal noise. The resulting number of exceeds is counted in threshold cycle (C_t) values (or quantification cycle (C_q) values according to the MIQE guidelines).

Cells were seeded at a cell count of approximately 2.5x 10^4 cells/well and 1 ml of cell medium was added.
After 3 days in culture, total RNA was isolated from the cells with the RNeasy Mini Kit (Qiagen, Hilden, Germany) according to the manufacturer's manual.

RNeasy Mini Kit protocol:

Things to consider:

□ Always work as clean as possible. Every fluid and vapor is a potential RNase-containing contaminant!

Prepare the following:

□ Mercaptoethanol
□ RNeasy Mini Kit (Qiagen) – for ingredients see the manufacturer's instruction
□ Ethanol 70%
□ 16x reaction tubes
□ 16x reaction tubes pre-filled with 250µl of 70% ice-cold ethanol
□ 16x RNeasy spin columns
□ Cell culture plates (2.5x 10^4cells/well/cell-type, cultured for 3 days - Low-Attachment 24-well plates incl. samples, TPP 24-well plates incl. control)

Procedure:

- Mix mercaptoethanol and RLT-buffer in a 50ml Falcon tube = **Lysis buffer** (10µl ME per 1ml RLT-buffer) > required total volume depends on the well size and number of wells (total volume = 80µl ME + 8ml RLT-buffer)
- Dispose of CM in the culture's wells (4 wells of the same material and cell-type at a time = 1 pooled sample)
- Add 1ml of PBS 1x to each of the 4 wells for washing and dispose of the PBS in the 1st well
- Add 350µl of Lysis buffer directly onto the washed cells and shake lightly to distribute the buffer (if available and applicable, use cellscraper to remove cells from the well's bottom)
- Dispose of the PBS in the 2nd well and transfer the suspension from the 1st well into the 2nd well, shake lightly again
- Continue procedure until the suspension has been transferred into the 4th well
- Transfer the whole suspension into the pre-labeled reaction tube containing Ethanol, shake lightly
- Continue procedure for the other samples
- Once all of the samples have been transferred into the reaction tubes, use a 1000µl pipette (set at 700µl) to transfer the samples into the pre-labeled RNeasy spin columns.
- Place the spin columns in a centrifuge at 10.000rpm for 30 sec
- Dispose of the collection tube's (CT) content

- Add 700µl of RW1-buffer to each spin column
- Centrifuge at 10.000rpm for 30 sec
- Dispose of the CT's content
- Add 500µl of RPE-buffer (RPE-buffer must be mixed with ethanol in order to be actived!)
- Centrifuge at 10.000rpm for 30 sec
- Dispose of the CT's content
- Centrifuge at 10.000rpm for 2 min
- Transfer each spin column into a clean CT
- Centrifuge for 1 min at full speed
- Transfer each spin column into a 1.5ml pre-labeled reaction tube (Labeling: e.g. RNA I hFOBa T SB)
- Add **30µl** of RNase-free water to each spin column
- Centrifuge at 10.000rpm for 1 min
- Dispose of spin column
- Instantly deep-freeze the reaction tubes at -80°C

Quantity of the extracted RNA was first measured as optical density (OD) 260/280 in a biophotometer system (BioPhotometer 6131, Eppendorf AG, Hamburg, Germany). RNA purity was estimated through the ratio between the absorbance values at 260 and 280 nm. RNA with a ratio above 1.8 and an estimated RNA concentration of above 30ng/µl was subsequently verified and tested on purity in the Agilent 2100 Bioanalyzer™ using the Agilent RNA 6000 Nano Kit (both Agilent Technologies, Santa Clara, CA). Apart from quantification, the so-called RNA Integrity number (RIN) was determined in this step. RIN estimation allows the classification of the degradation rate of total RNA in a sample and is based on a numbering system from 1 to 10, with 1 being the most degraded and 10 being the most intact. All values above 7 were rendered suitable for further qPCR analysis.

Before proceeding with qPCR, 1µg of RNA per sample was purified with DNase-I treatment (Thermo Scientific, Waltham, MA) and reverse-transcribed into cDNA applying the iScript cDNA Synthesis Kit (Bio-Rad Laboratories, Hercules, CA):

Removal of genomic DNA (Thermo Scientific #EN0521):

(Volumes per sample, each run consists of 37 samples)	
RNA 1µg (add up to 8µl)	xµl
10x reaction buffer with $MgCl_2$	1µl
DNAse I, RNase-free	1µl
Diethylpyrocarbonate (DEPC)-treated water	xµl
	10µl

- Mix ingredients in a 0,5ml reaction tube/sample
- Incubate all samples at. 37°C for 30 min in a thermocycler
- Add 50mM/1µl of Ethylenediaminetetraacetic acid (EDTA)
- Incubate at 65°C for 10 min in a thermocycler

cDNA synthesis with the iSCript cDNA Synthesis Kit (Bio-Rad, #170-8891, 100rxn)

(Volumes per sample, each run consists of 37 samples)	
5x iScript reaction mix	4µl
iScript reverse transcriptase[1]	1µl
NFW (nuclease-free water)	4µl
RNA template[2]	11µl
	20µl

Thermocycler reaction protocol:

5 min	25°C
30 min	42°C
5 min	85°C
Hold at	4°C

[1] For RT-, substitute iScript reverse transcriptase was for additional 1µl of NFW

[2] For Control, substitute RNA template for additional 11µl of NFW

Sso-Advanced™ Universal SYBR®Green supermix (Bio-Rad) was added as a non-specific DNA-binding fluorescence dye plus mastermix and amplification was conducted on the Bio-Rad® CFX96™ system (Bio-Rad). Each qPCR run consisted of a standard 3-step PCR temperature protocol (annealing temperature of 60°C) followed by a melting curve protocol to confirm a single gene-specific peak and to detect primer dimerization.
The primers used for RT-qPCR included QuantiTect primer assays (Qiagen) for proliferating cell nuclear antigen (PCNA, ID QT00024633), marker of proliferation Ki-67 (MKI67, ID QT00014203) and Vinculin (VCL, ID QT00078302).

Detailed qPCR protocol:

(Volumes per sample, each run consists of 37 samples)	
SsoAdvanced™ universal SYBR® Green supermix 2x	30µl
Quantitect Primer 10x	6µl
NFW	21µl
Template (6,25ng/µl)[3]	3µl
	60µl

- First, pre-fill the 0.5 ml reaction tubes with NFW + Primer, then add the template to the side of the cuvette, close, spin the reaction tube in a centrifuge once, then add the SYBR Green supermix, vortex again and spin again.
- After mixing, pipette 19µl/well into a 96-well plate designed for qPCR according to the schematic (refer to Table 3 for schematics, 3 wells/sample, avoid bubbles!).
- Before being placed in the Bio-Rad® CFX96™ thermocycler the plate is centrifuged at 900rpm for 1 min (refer to Fig.10 for thermocycler protocol).

[3] For NTC, substitute Template for additional 3µl of NFW

	1	2	3	4	5	6	7	8	9	10	11	12
A	GAPDH KO	GAPDH KO	GAPDH KO	HPRT KO	HPRT KO	HPRT KO	PCNA KO	PCNA KO	PCNA KO	GAPDH NTC	GAPDH NTC	GAPDH NTC
B	GAPDH cp-Ti	GAPDH cp-Ti	GAPDH cp-Ti	HPRT cp-Ti	HPRT cp-Ti	HPRT cp-Ti	PCNA cp-Ti	PCNA cp-Ti	PCNA cp-Ti	ACTB NTC	ACTB NTC	ACTB NTC
C	GAPDH PEEK	GAPDH PEEK	GAPDH PEEK	HPRT PEEK	HPRT PEEK	HPRT PEEK	PCNA PEEK	PCNA PEEK	PCNA PEEK	HPRT NTC	HPRT NTC	HPRT NTC
D	GAPDH Y-TZP	GAPDH Y-TZP	GAPDH Y-TZP	HPRT Y-TZP	HPRT Y-TZP	HPRT Y-TZP	PCNA Y-TZP	PCNA Y-TZP	PCNA Y-TZP	VCL NTC	VCL NTC	VCL NTC
E	ACTB KO	ACTB KO	ACTB KO	VCL KO	VCL KO	VCL KO	MKI67 KO	MKI67 KO	MKI67 KO	PCNA NTC	PCNA NTC	PCNA NTC
F	ACTB cp-Ti	ACTB cp-Ti	ACTB cp-Ti	VCL cp-Ti	VCL cp-Ti	VCL cp-Ti	MKI67 cp-Ti	MKI67 cp-Ti	MKI67 cp-Ti	MKI67 NTC	MKI67 NTC	MKI67 NTC
G	ACTB PEEK	ACTB PEEK	ACTB PEEK	VCL PEEK	VCL PEEK	VCL PEEK	MKI67 PEEK	MKI67 PEEK	MKI67 PEEK	RT-	RT-	RT-
H	ACTB Y-TZP	ACTB Y-TZP	ACTB Y-TZP	VCL Y-TZP	VCL Y-TZP	VCL Y-TZP	MKI67 Y-TZP	MKI67 Y-TZP	MKI67 Y-TZP	Control	Control	Control

Reference genes

Genes of interest

Primer control (no cDNA- template added for qPCR)

RT – (no reverse transcriptase added for cDNA synthesis)

Control (no RNA template added for cDNA synthesis)

Table 4: Schematics for 96-well plate in qPCR measurement.

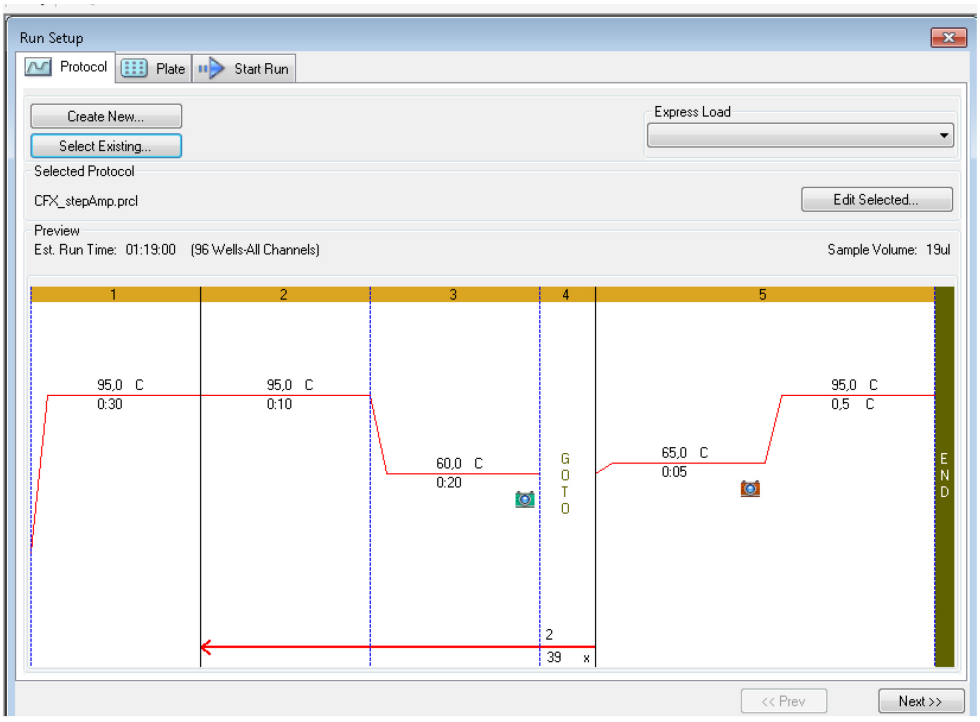

Figure 10: Bio-Rad® CFX96™ reaction protocol.

Relative quantification of expression levels was obtained by the $\Delta\Delta C_t$ method based on the geometric mean of the internal reference genes glyceraldehyde 3-phosphate dehydrogenase (GAPDH, ID QT00079247), β-actin (ACTB, QT00095431), and hypoxanthine phosphoribosyl-transferase (HPRT-1,QT00059066), respectively.

The expression level C_t of the target gene was normalized to the reference genes (ΔC_t), the ΔC_t of the test sample was normalized to the ΔC_t of the control ($\Delta\Delta C_t$). Finally, the expression ratio was calculated with the $2^{-\Delta\Delta Ct}$ method (* $p < 0.05$).

2.6 Scanning electron microscopy (SEM)

2.5x 10^4 cells were seeded into each well of 24-well Low Attachment plates pre-assembled with material disks and kept under the above mentioned culture conditions.

On day 3, the medium was removed and the samples were immediately fixated inside the well with 2.5% (wt/vol) glutaraldehyde and 2% (wt/vol) paraformaldehyde in 0.1M cacodylate buffer for 30 min at room temperature. Samples were then rinsed in 0.1M cacodylate buffer for 3 hours, then post-fixed for 30 min in 2% (wt/vol) osmium tetroxide and rinsed again in cacodylate buffer. After dehydration in a graded series of 30-100% ethanol (30 min/step), samples in super-dry ethanol were rinsed in 100% acetone for 5 min, critically point dried, mounted on aluminum pins and sputter coated with gold and palladium. Cells were analyzed in a scanning electron microscope (ZeissDSM 950; Carl Zeiss, Oberkochen, Germany).

2.7 Immunofluorescence staining

Two cytoskeletal proteins were designated for immunofluorescence (IF) staining.

First, the mesenchymal intracellular intermediary filament Vimentin was selected for verifying the mesenchymal origin of the cultured cells (38).

Second, the cytoskeletal protein Vinculin, an attachment protein involved in the indirect binding of intracellular actin filaments to extracellular fibronectin, was chosen to illustrate cellular attachment to the extracellular matrix (39).

2.5x 10^4 cells/cell-type were seeded into each well on 24-well Low Attachment plates pre-assembled with material disks as described above. For positive control, HELA, hFOB and hGF cells were seeded at a cell count of 2.5x 10^4 cells/chamber on regular four-chamber slides and cultivated simultaneously for 3 days under conditions appropriate to each cell type (culture conditions as instructed by manufacturer, refer to Fig. 12 for seeding schematics).

After 3 days in culture, all wells and chambers were washed with 1ml of PBS 1x, air dried and stored at -20°C until IF was carried out.

Subsequently, cells were labeled with monoclonal mouse antibody to either human Vimentin (DAKO, Vienna, Austria) or Vinculin (Thermo Scientific). As secondary antibody, Cy-2™ conjugated goat-anti mouse antibody (Jackson Immuno Research, Baltimore, PA) was used, resulting in a green fluorescent color. Briefly, cells were fixated with 4% formaldehyde in PBS for 10 minutes. After washing step with PBS, the samples were blocked with UltraVision Protein Block (Thermo Scientific) and incubated with the primary antibody for 30 min at room temperature. The biomaterial samples were washed three times in PBS and incubated light-protected with secondary antibody for 30 min at room temperature. Vectashield® mounting medium containing DAPI dye (Vector Laboratories, Burlingame, CA) was used for core staining. Samples were analyzed by confocal laser scanning microscopy (Zeiss LSM 510 META; Carl Zeiss, Oberkochen, Germany).

Detailed protocol for Immunofluorescence staining:

Things to consider:

- □ 2nd antibody is susceptible to light – staining and incubation should be conducted under minimum lighting conditions
- □ 14mm disks of the investigated materials must be cultivated on Low-Attachment 24-well plates, transferred onto regular 24-well plates for staining and placed on special laboratory equipment, designed for the LSM-510 microscope – cautious handling is required at all times (preferably, disks should be transferred deploying tweezers made from plastic and only be touched on the edges to avoid mechanical cellular detachment before analysis)
- □ No staining is applied to the autofluorescence-wells after disk transfer!
- □ HeLa cells served as a positive control
- □ Anti-mouse IgG served as a negative control

Prepare the following:

- ☐ 4% wt/vol Formaldehyde diluted PBS 1x (pFA)
- ☐ Antibody dilutent (AB-dil) containing 1% wt/vol bovine serum albumin (BSA) + 0,3% wt/vol Triton X-100 buffer in PBS 1x
- ☐ 1st antibodies:
  - Diluted Vimentin Antibody (VIM-AB, Clone V9, #M0725, lot: 20013519, 156µg/ml, DAKO)
  - Diluted Vinculin Antibody (VIN-AB, Clone VLN01, #MS-1209-P1, lot:1209P105I, 200µg/ml: 0,5ml, Thermo Fisher Scientific)
- ☐ Diluted monoclonal Mouse IgG (Cat. No CAM2001AB, lot: 200103, 1mg/ml, LINARIS GmbH, Dossenheim, Germany), as a negative control
- ☐ 2nd antibody:
  - Diluted Anti-mouse AB (Cy-2, Cy-2™ conjugated Goat anti-mouse, #155-225-003, lot: 102983, 2mg, 1,5mg/ml, Jackson ImmunoResearch)
- ☐ Mounting medium (MM, Vectashield Mounting Medium with DAPI, #H-1200, Vector Laboratories)
- ☐ UltraVision Protein Block (PB, #TA-125-PBQ, lot: PBQ 141209, Thermo Fisher Scientific)

Procedure:

- For IF staining frozen sample disks were transferred to a regular TPP 24-well plate using tweezers (Attention: Cells should never dry after fixation!). Disks were placed into the wells designated on the schematic below:

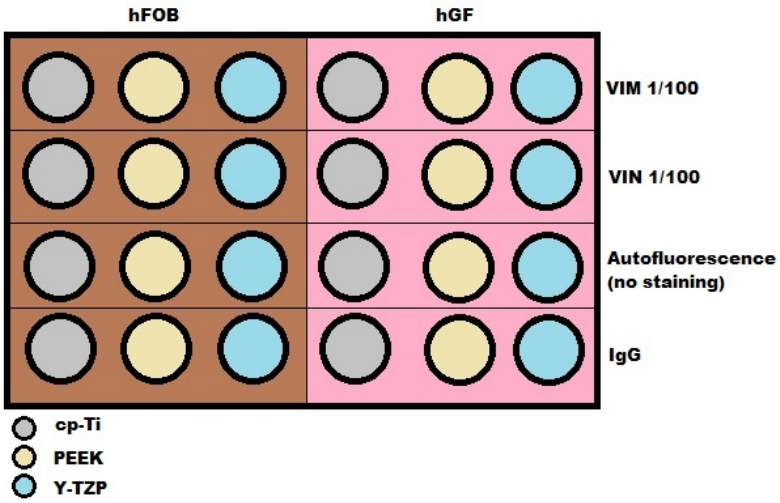

Figure 11: Schematic for IF staining on material disks.

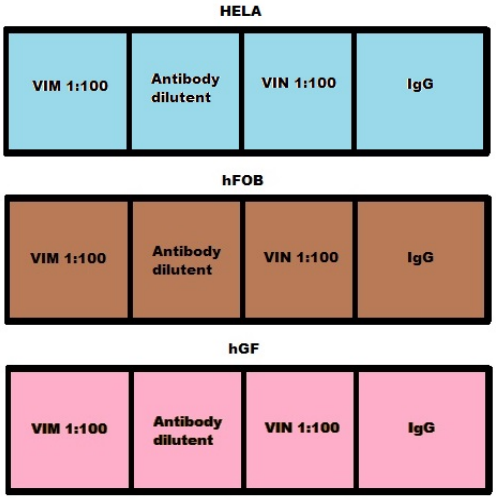

Figure 12: Schematic for IF staining of controls on chamber slides.

- Disks and control slides were fixated with 4% pFA for approx. 10 min at room temperature
- To remove 4% pFA, cells were washed with PBS 1x for 5 min
- Non-specific binding was prevented by adding five drops of blocking buffer to each well/chamber. Exceeding buffer was disposed after an incubation of 5 min at room temperature
- 300µl of VIM 1:100, VIN 1:100, AB-dil, or Mouse IgG were added to each well/chamber (according to the schematics above) and incubated for 30 min at room temperature
- All wells were washed with PBS 1x for 3 times (5 min each)
- WORK UNDER LOW-LIGHT CONDITIONS FROM HEREON!
- PBS 1x was discharged and 300µl of Cy-2 1:100 was added to each well/chamber and incubated for 30 min at room temperature under light-protection
- All wells were washed with PBS 1x for 3 times (5 min each)
- Each well/chamber was counterstained and embedded with H-1200 Vectashield MM for approximately 1 min
- Samples and positive control were instantly investigated under the LSM-510 for best results

2.8 Statistical methods

All values are expressed as mean ± standard deviation. Student's unpaired *t*-test was used to evaluate differences between the groups and their respective controls. To determine the change over time a one-way ANOVA was calculated for each group. The difference in the increase of the slopes was determined. All statistic tests and graphic data were prepared in SPSS™ 22 (IBM Statistics, Armonk, NY).

3 Results

3.1 Cell line characterization

As described above, a standardized hFOB cell line was used in this study and compared to the data provided by ATCC® through short tandem repeat (STR) analysis. In the hGF cells, we compared two separate passages (p6 and p9) as this cell line was a primary cell line and no detailed data was provided by the company.

DNA profiles were similar to the respective control in both cell lines (refer to tables 4 and 5 for detailed gene loci).

STR locus	hFOB p13	Data provided by ATCC®
D3S1358	17, 18	
TH01	7, 9.3	7, 9.3
D21S11	29, 32.2.	
D18S51	10, 17	
Penta E	8, 11	
D5S818	11, 12	11, 12
D13S317	11, 12	11, 12
D7S820	8, 10	8,10
D16S539	9, 13	9, 13
CSF1PO	10, 11	10, 11
Penta D	9, 13	
Amelogenin	X	X
vWA	16, 18	16, 18
D8S1179	10, 14	
TPOX	11	11
FGA	19, 22	

Table 5: STR profile of passage 13 hFOB cells is equal to the profile provided by ATCC®.

STR locus	hGF p6	hGF p9
D3S1358	16, 17	16, 17
TH01	6, 9	6, 9
D21S11	29, 30	29, 30
D18S51	12, 18	12, 18
Penta E	7, 19	7, 19
D5S818	12, 13	12, 13
D13S317	11	11
D7S820	11	11
D16S539	11	11
CSF1PO	10, 11	10, 11
Penta D	13	13
Amelogenin	X	X
vWA	15, 16	15, 16
D8S1179	8, 13	8, 13
TPOX	8, 11	8, 11
FGA	19, 27	19, 27

Table 6: STR profile of passage 6 and 9 hGF cells showed equal results.

Further characterization of hFOB and hGF cell lines was accomplished through IF staining of the mesenchymal marker Vimentin after 3 days of cultivation at an initial cell density of 2.5x 10^4 cells/well.

As shown in Fig. 13 A to C, both cell lines exhibited equal intensity of cytoplasmatic Vimentin staining when compared to positive control HeLa cells, identifying both cell types as adhesive cells of mesenchymal origin.

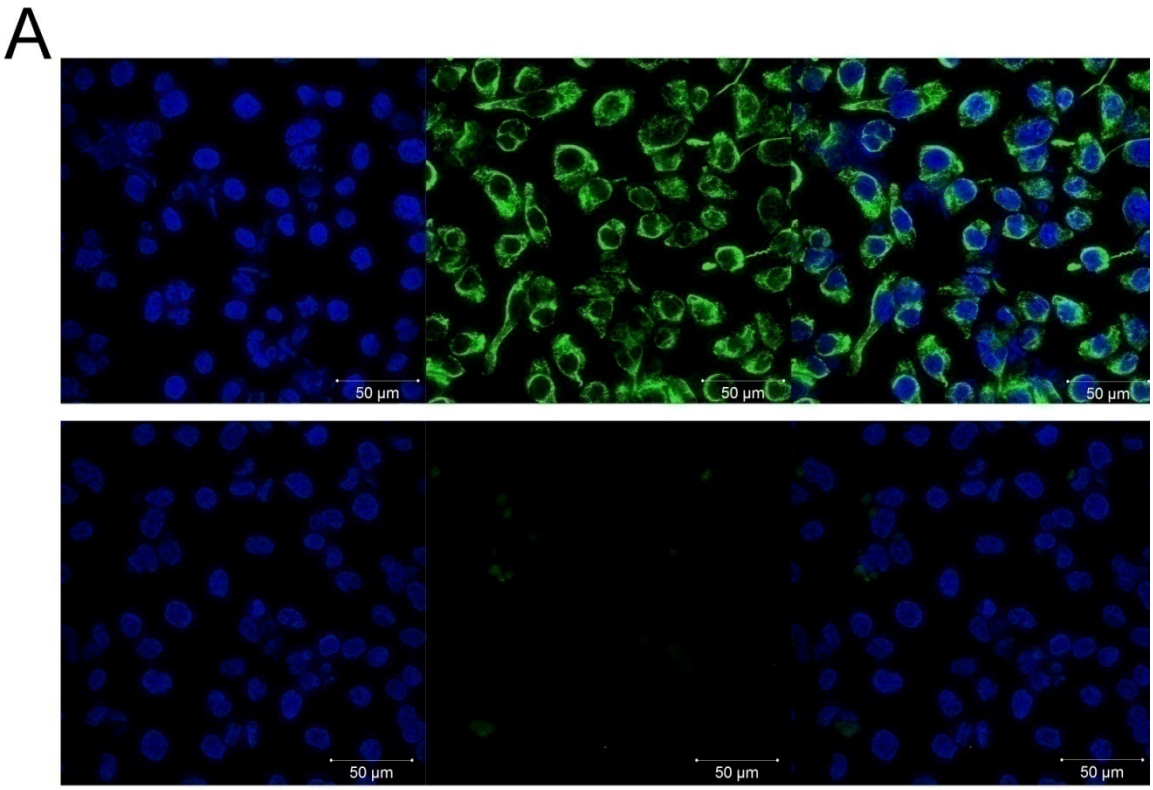
A
50 µm
50 µm
50 µm
50 µm
50 µm
50 µm

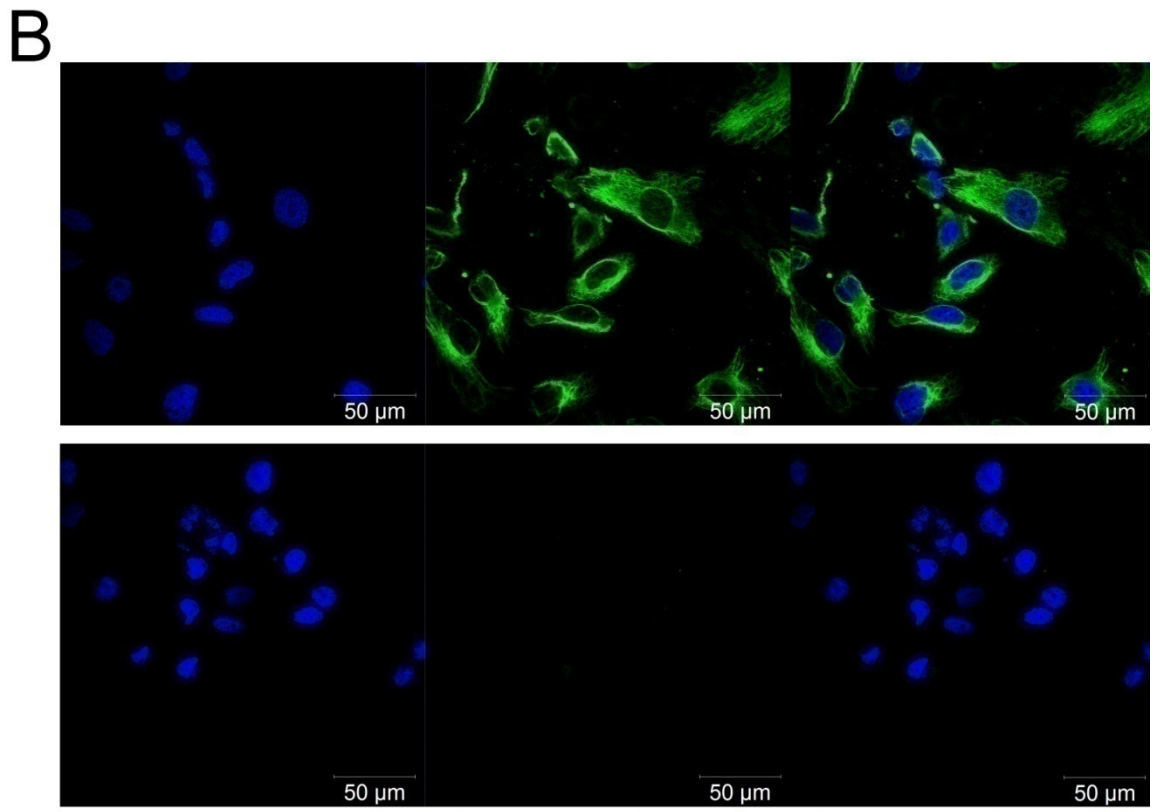
B
50 µm
50 µm
50 µm
50 µm
50 µm
50 µm

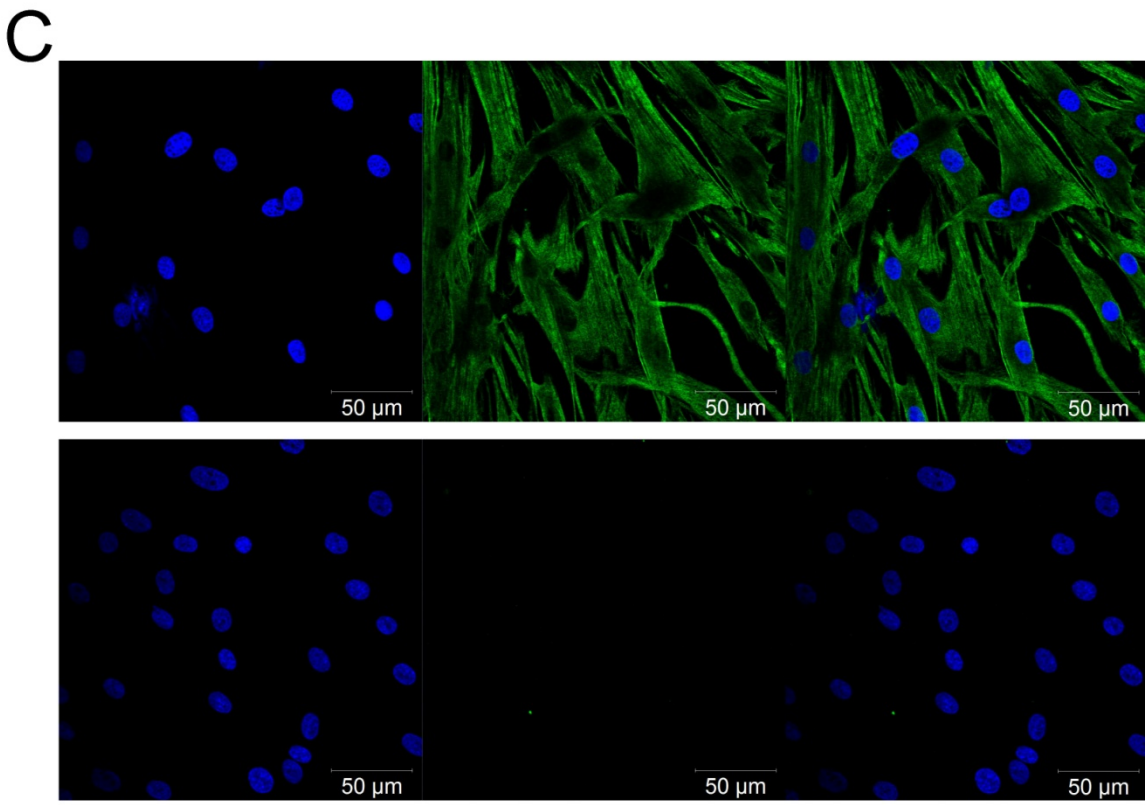

Figure 13: Fluorescent staining images showing the expression of the mesenchymal cytoplasmatic marker Vimentin in A) HeLa, B) hFOB, and C) hGF cells after 3 days of culture. Mouse IgG negative control of each specimen is shown in boxes below. Original magnification x200; bar = 50 µm.

3.2 Cell viability and proliferation analysis

On day 1, 3 and 7 the metabolic activity was measured applying the MTS assay. As described above, regular polystyrene cell culture plates were used as control material. The initial cell density was 1.5x 10^4 cells/well.

In hFOB cells (passage 15, n=4-6), statistical analysis showed significant differences in all 3 groups on each separate day. Cp-Ti and Y-TZP exhibited almost the same reduction of viability on each day, while PEEK performed worst on each single day (Table 6 and Fig. 13 A). In each group, the changes in the slope value showed only a slight significance in PEEK on day 1 when compared to day 3. (p=0.028, Fig. 13 B)

hFOB		Control	cp-Ti	PEEK	Y-TZP
Day 1	Number of experiments (n)	4	4	4	4
	Mean ± SD (% of control)	100	54.9±8.9	41.8±17.3	59.4±11.6
	p-value (unpaired t-test)		0	0.001	0
Day 3	Number of experiments (n)	5	5	5	5
	Mean ± SD (% of control)	100	75.1±12.8	68.5±10.7	78.6±13.4
	p-value (unpaired t-test)		0.002	0.003	0.024
Day 7	Number of experiments (n)	6	6	6	6
	Mean ± SD (% of control)	100	62.5±11.6	52.2±12.3	70.8±18.2
	p-value (unpaired t-test)		0.001	0	0.011

Table 7: Detailed data for MTS assay in hFOB cells.

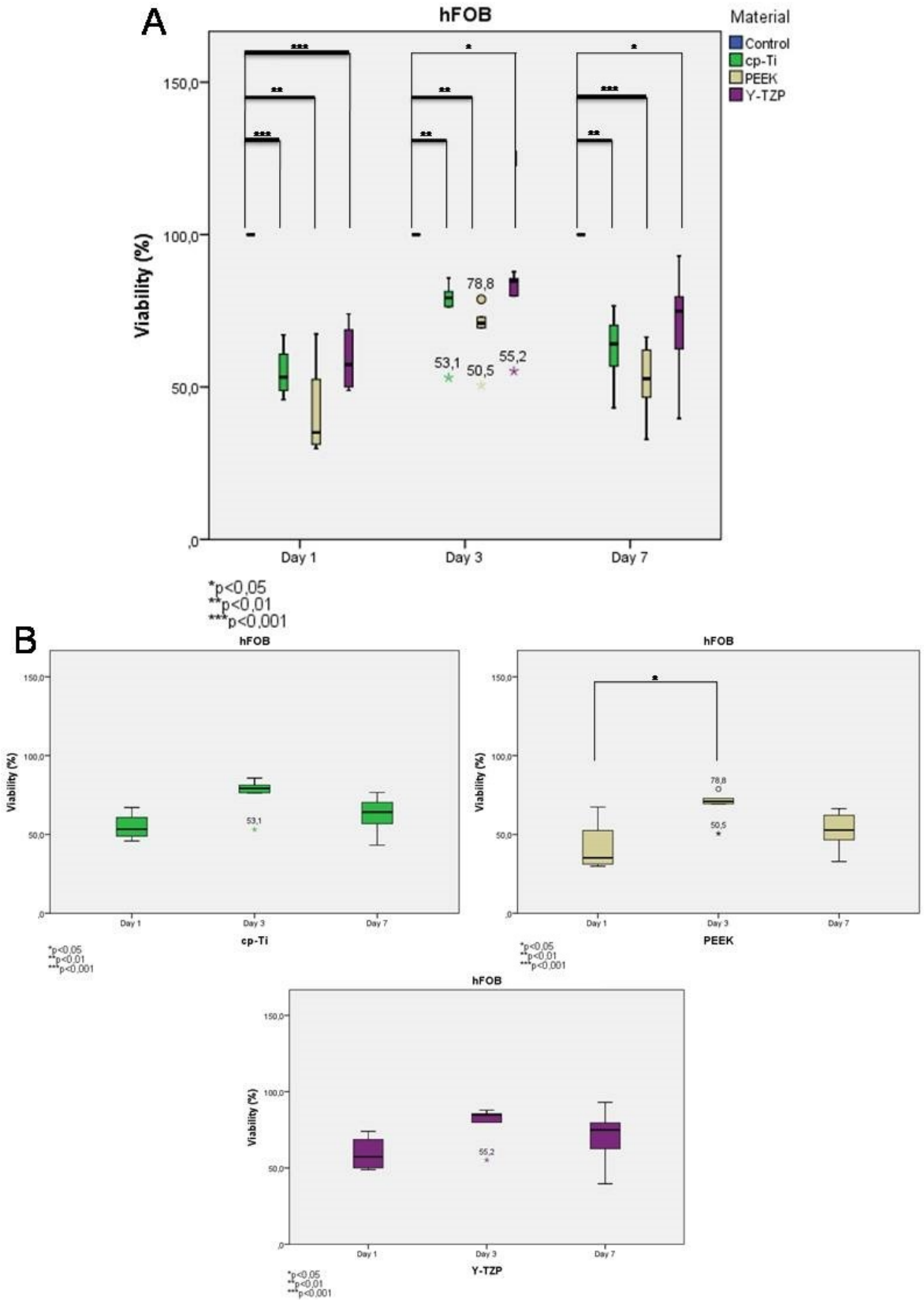

Figure 14: Results of the MTS assay analysis in hFOB cells seeded on 3 different dental materials. Cellular viability of cells was measured after A) one, three and seven days of culture and normalized to the value of the cell culture in polystyrene 24-well plates (100%). B) Viability over time in each group is displayed separately. All box blots represent the median values with the 75th and 25th percentile, extraordinary and extreme values. Significant p-values are designated in brackets above.

In hGF cells (passage 9, n=5), growth patterns painted a similar picture with cp-Ti and Y-TZP again performing almost equally over time and in-between groups. While both materials even managed to outperform control on days 3 and 7, PEEK again demonstrated a significant reduction in viability on each day when compared to control (Table 7 and Fig. 14 A).

In each groups, significant changes in slope values were observed between days 1-3 and 1-7 in each group (Fig. 14 B).

hGF		Control	cp-Ti	PEEK	Y-TZP
Day 1	Number of experiments (n)	5	5	5	5
	Mean ± SD (% of control)	100	73.8±6.3	55.3±5.1	82±11.5
	p-value (unpaired t-test)		0.001	0	0.008
Day 3	Number of experiments (n)	5	5	5	5
	Mean ± SD (% of control)	100	97.6±15.2	78.8±14.7	106.2±19.2
	p-value (unpaired t-test)		0.74	0.032	0.511
Day 7	Number of experiments (n)	5	5	5	5
	Mean ± SD (% of control)	100	103±12.8	74.1±8.5	114.6±10.8
	p-value (unpaired t-test)		0.623	0.002	0.039

Table 8: Detailed data for MTS assay in hGF cells.

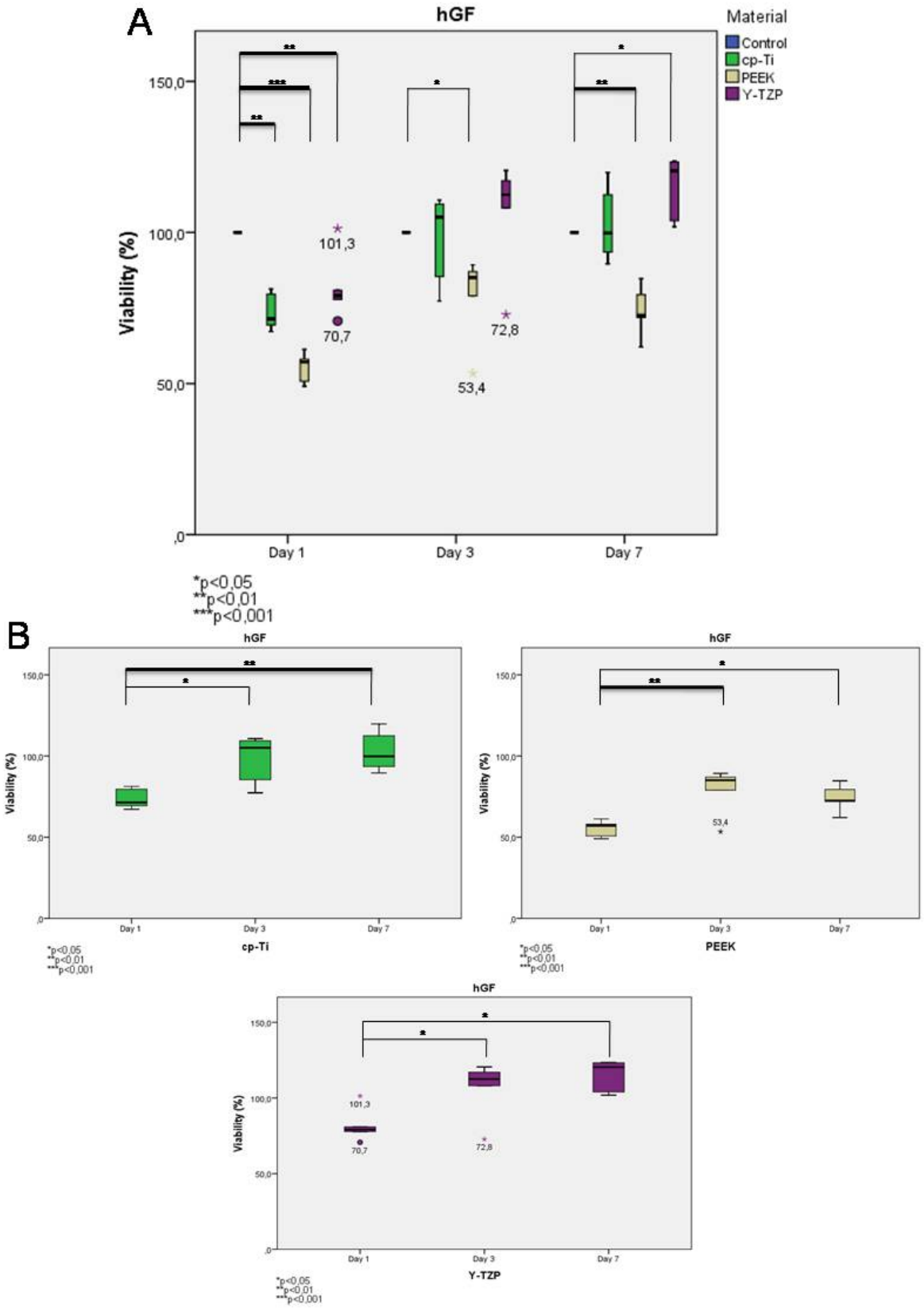

Figure 15: Results of the MTS assay analysis in hGF cells seeded on 3 different dental materials. Cellular viability of cells was measured after A) one, three and seven days of cultivation and normalized to the value of the cell culture in polystyrene 24-well plates (100%). B) Viability over time in each group is displayed separately. All box blots represent the median values with the 75th and 25th percentile, extraordinary and extreme values. Significant p-values are designated in brackets above.

To measure a potential induction of proliferation by each material, we determined the relative mRNA expression levels of the proliferation markers Ki67 and PCNA after 3 days in culture through RT-qPCR. Cells were seeded at an initial cell density of 2,5x 10^4 cells/well. The polystyrene control group served as the reference value (ratio = 1). Values were mean ± SD of independent experiments performed in triplicates.

In hFOB cells (p15, n=4-5), both PCNA and Ki67 showed no significant differences in gene expression in the groups when compared to control (Fig. 15 A).

In hGF cells (p9, n=5-6), only cp-Ti revealed a slight significance in the expression of Ki67 ($p=0.026$) (Fig. 15 B).

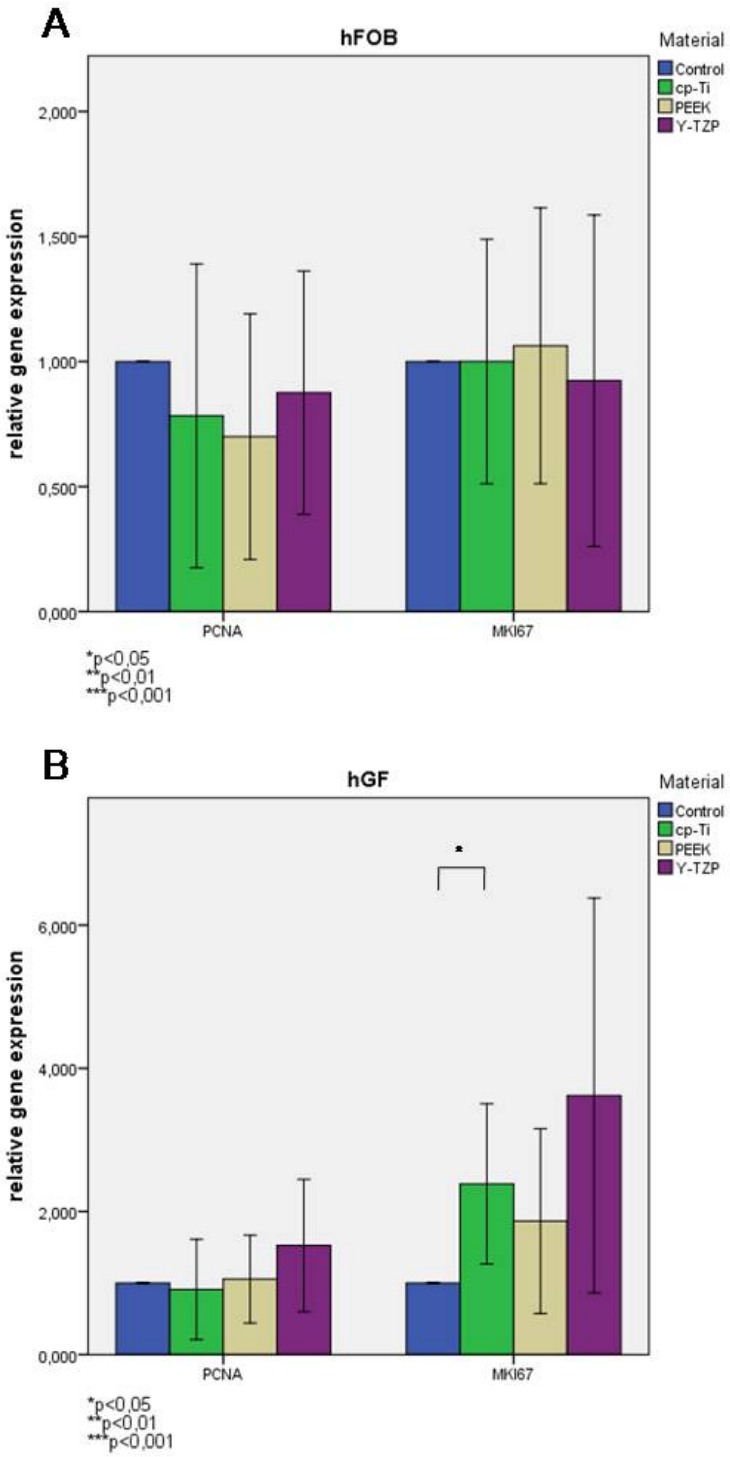

Figure 16: Ki67 and PCNA expression were analyzed at mRNA levels in both A) hFOB and B) hGF cells seeded on different dental materials over a period of 3 days. Relative gene expression was measured by RT-PCR and normalized on reference genes ($2^{-\Delta\Delta Ct}$-method). Data is shown as mean ± SD. Significant p-values are designated in brackets above.

3.3 Cytotoxicity

Cytotoxicity was determined through LDH measurement on days 1, 3 and 7.

The initial cell density was 1,5x 10^4 cells/well.

In hFOB cells (p15, n=4-7), only slight significant changes were found on day 1 and day 7 when compared to control (Table 8 and Fig. 16 A), but overall cytotoxicity remained stable in all three groups.

A significant increase in LDH-levels was revealed over time in each separate group (Fig. 16 B).

hFOB		Control	cp-Ti	PEEK	Y-TZP
Day 1	Number of experiments (n)	4	4	4	4
	Mean ± SD (% of MAX-wells)	17±2	11.1 ±2.3	11.4±3	11.1±3.5
	p-value (unpaired t-test)		0.009	0.022	0.027
Day 3	Number of experiments (n)	7	7	7	7
	Mean ± SD (% of MAX-wells)	29.5±7.3	20.8±6.8	26.3±5.1	27.7±9.4
	p-value (unpaired t-test)		0.04	0.364	0.694
Day 7	Number of experiments (n)	7	7	7	7
	Mean ± SD (% of MAX-wells)	36.1±6.3	29.9±11.7	23.7±9.2	33.4±7.8
	p-value (unpaired t-test)		0.246	0.012	0.491

Table 9: Detailed data for Cytotox assay in hFOB cells.

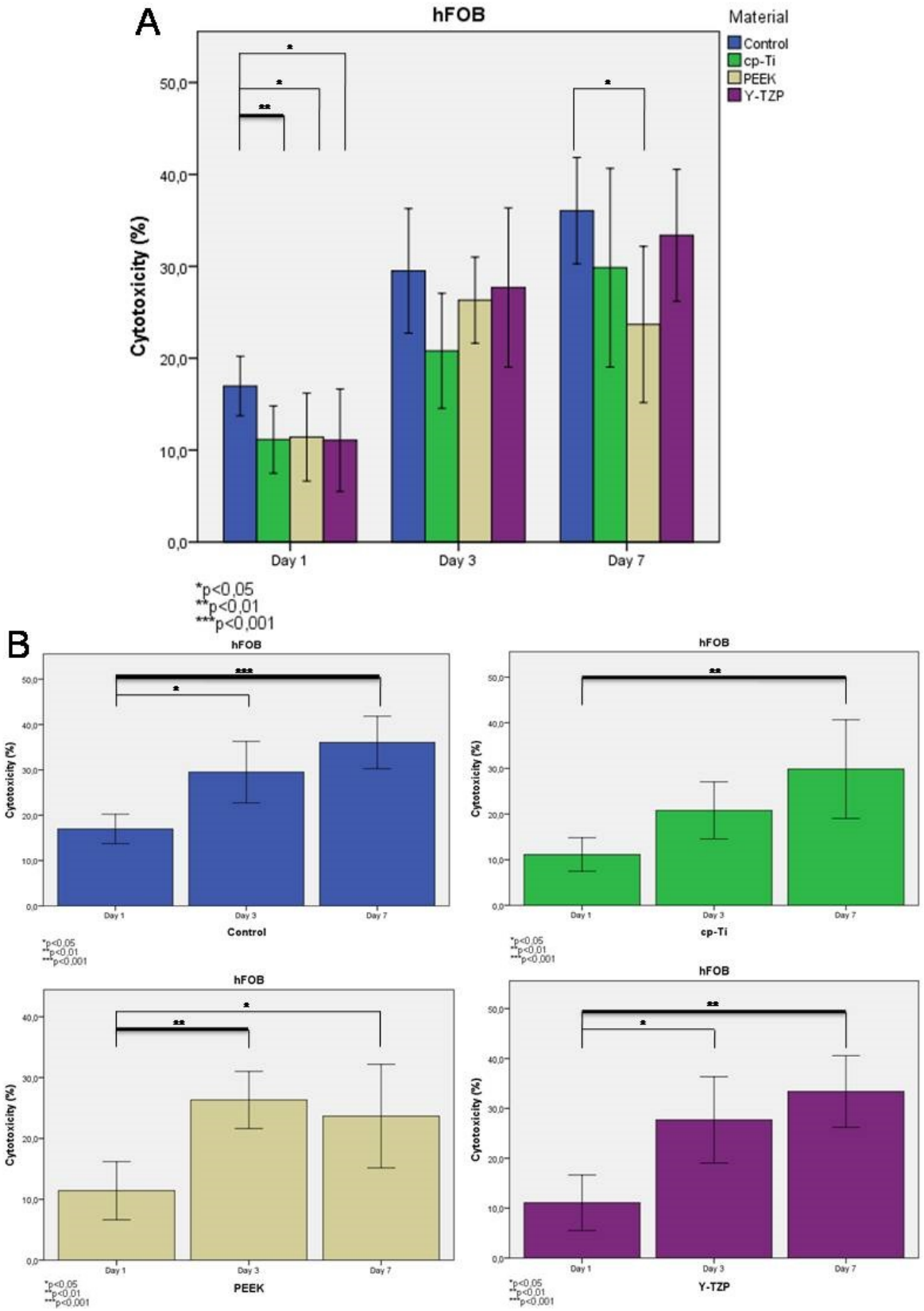

Figure 17: Results of the Cytotox assay analysis in hFOB cells seeded on 3 different dental materials. A) The LDH level of the supernatant was measured after one, three and seven days of cultivation. B) Cytotoxicity over time in each group is displayed separately. Data is shown as mean ± SD. Significant p-values are designated in brackets above.

In hGF cells (p9, n=5-6), LDH values remained on a similar level in all three groups when compared to control (Table 9 and Fig. 17 A).

Surprisingly, LDH values evenly decreased over time in all three groups. Also, each separate group showed a highly significant decrease in the slope value from day 1 to day 7 (Fig. 17 B).

hGF		Control	cp-Ti	PEEK	Y-TZP
Day 1	Number of experiments (n)	5	5	5	5
	Mean ± SD (% of MAX-wells)	10±0,8	9.6±1.8	11.2±1.7	11.9±1.5
	p-value (unpaired t-test)		0.643	0.174	0.039
Day 3	Number of experiments (n)	6	6	6	6
	Mean ± SD (% of MAX-wells)	6.3±2	6.6±1.9	7.5±2.2	7.9±2.5
	p-value (unpaired t-test)		0.772	0.326	0.245
Day 7	Number of experiments (n)	6	6	6	6
	Mean ± SD (% of MAX-wells)	4±1.9	3.5±1	3.2±0.7	4.8±1
	p-value (unpaired t-test)		0.525	0.329	0.413

Table 10: Detailed data for Cytotox assay in hGF cells.

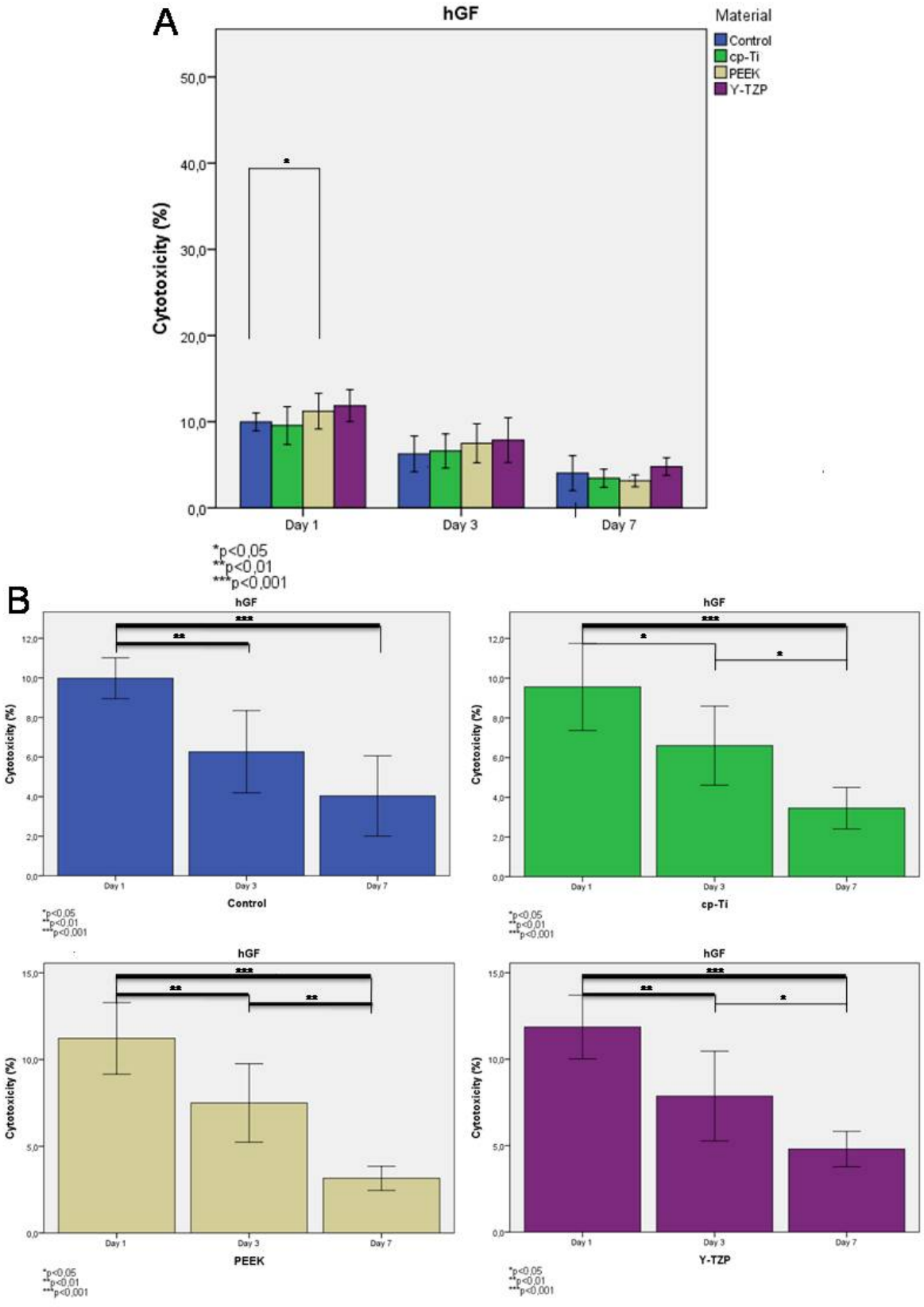

Figure 18: Results of the Cytotox assay analysis in hGF cells seeded on 3 different dental materials. A) The LDH level of the supernatant was measured after one, three and seven days of cultivation. B) Cytotoxicity over time in each group is displayed separately. Data is shown as mean ± SD. Significant p-values are designated in brackets above.

3.4 Morphological analysis

After 3 days in culture at an initial cell density of 2.5x 10^4 cells/well, cells of either hFOB or hGF were fixated and investigated under the scanning electron microscope (SEM). As shown on Fig. 18 A and B, both cell types attached and proliferated on all three materials, exhibiting cytoplasmatic extensions in all specimens. On cp-Ti and Y-TZP surfaces (left and right column), cell extensions appeared to be flat and star-shaped in both hFOB and hGF cells and the surfaces seem to be covered in what appears to be a deposition of extracellular matrix surrounding the cells.

On PEEK surfaces, both cell types appeared to be less numbered, were not surrounded by matrix and showed fewer extensions that resembled round-edged shapes similar to filopodia (Fig. 18 A and B, middle column).

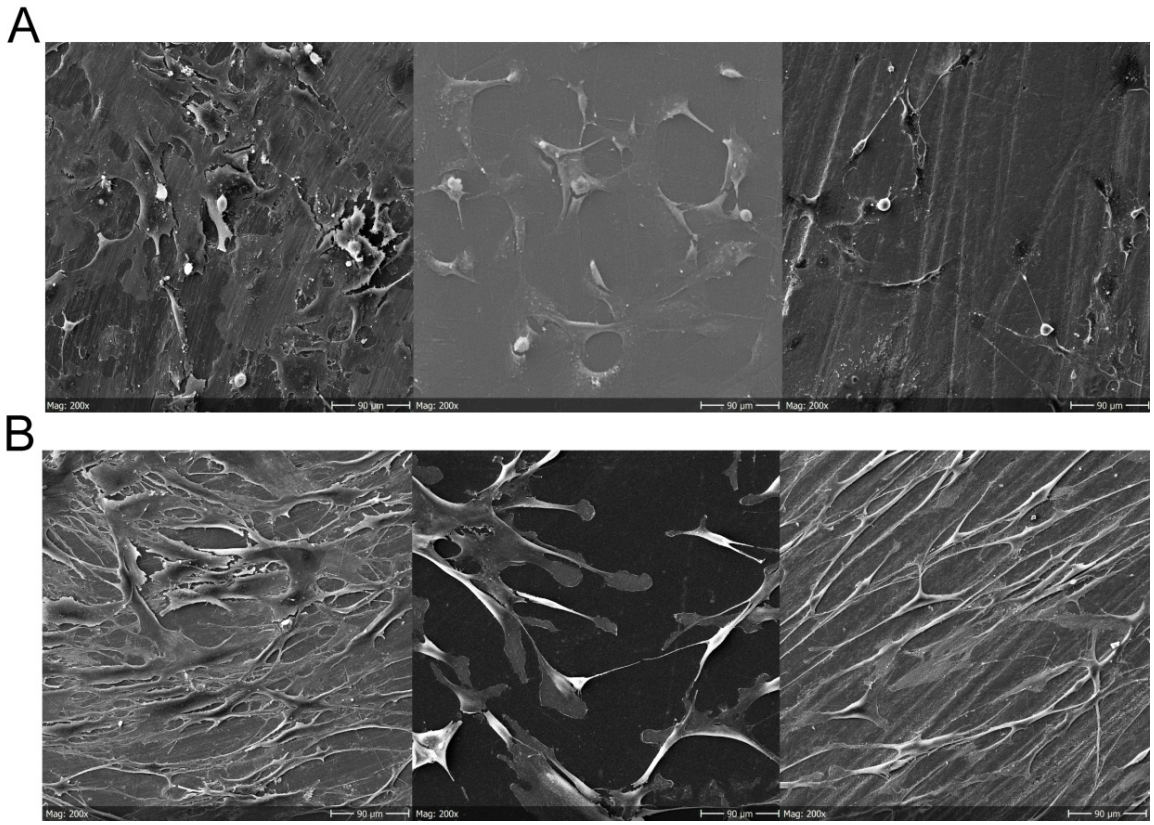

Figure 19: SEM images showing A) hFOB and B) hGF cells after 3 days of culture on cp-Ti, PEEK and Y-TZP disks. Original magnification x200; bar = 90 µm.

Immunofluorescence (IF) staining of the mesenchymal marker Vimentin showed similar images. In both hFOB and hGF cells, Vimentin was strongly expressed on cp-Ti and Y-TZP surfaces (as shown in Fig. 19 and 20, A to C, respectively). On PEEK, Vimentin staining was weaker than in the other groups and the cells exhibited round-edged cell borders and filopodia.

In both cp-Ti and PEEK surfaces, a high level of auto-fluorescence originating from the material itself was registered, most remarkably present in the negative control of each material and cell line (Fig. 19 and 20, A and B).

A

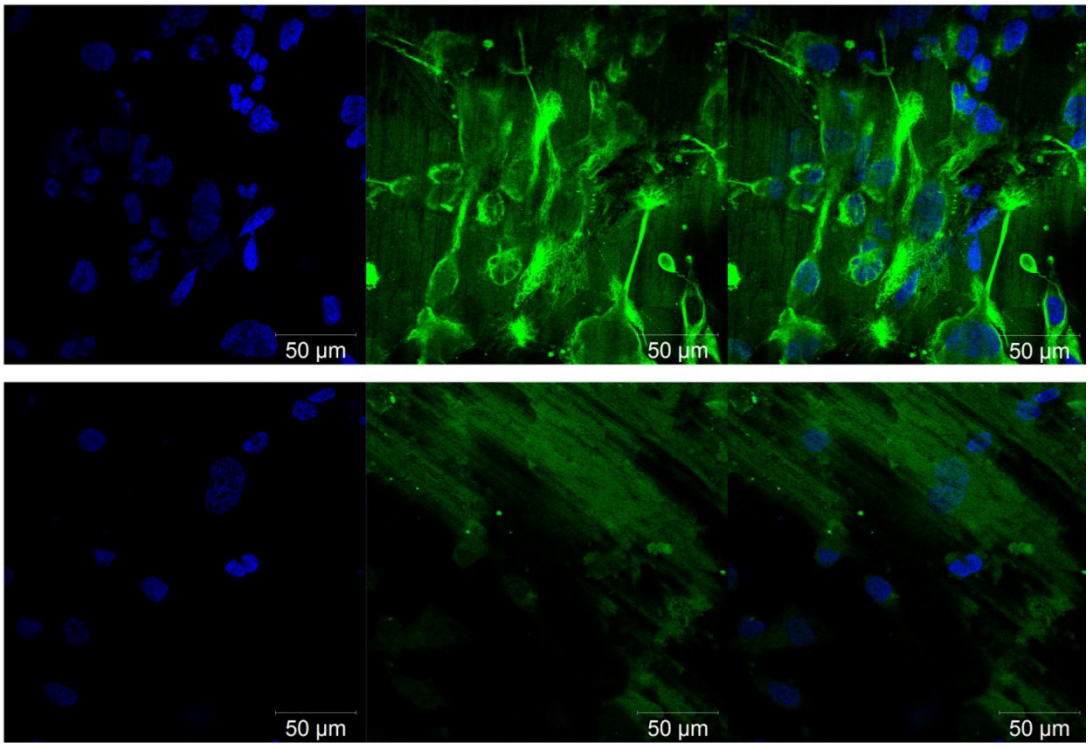

B

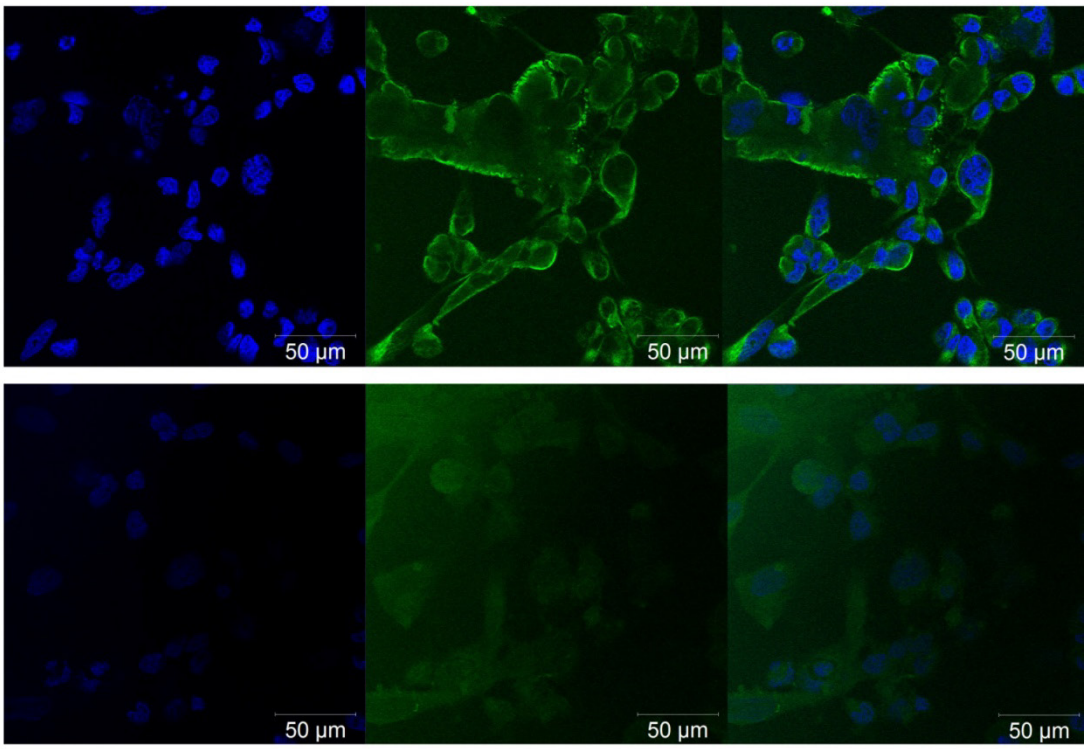

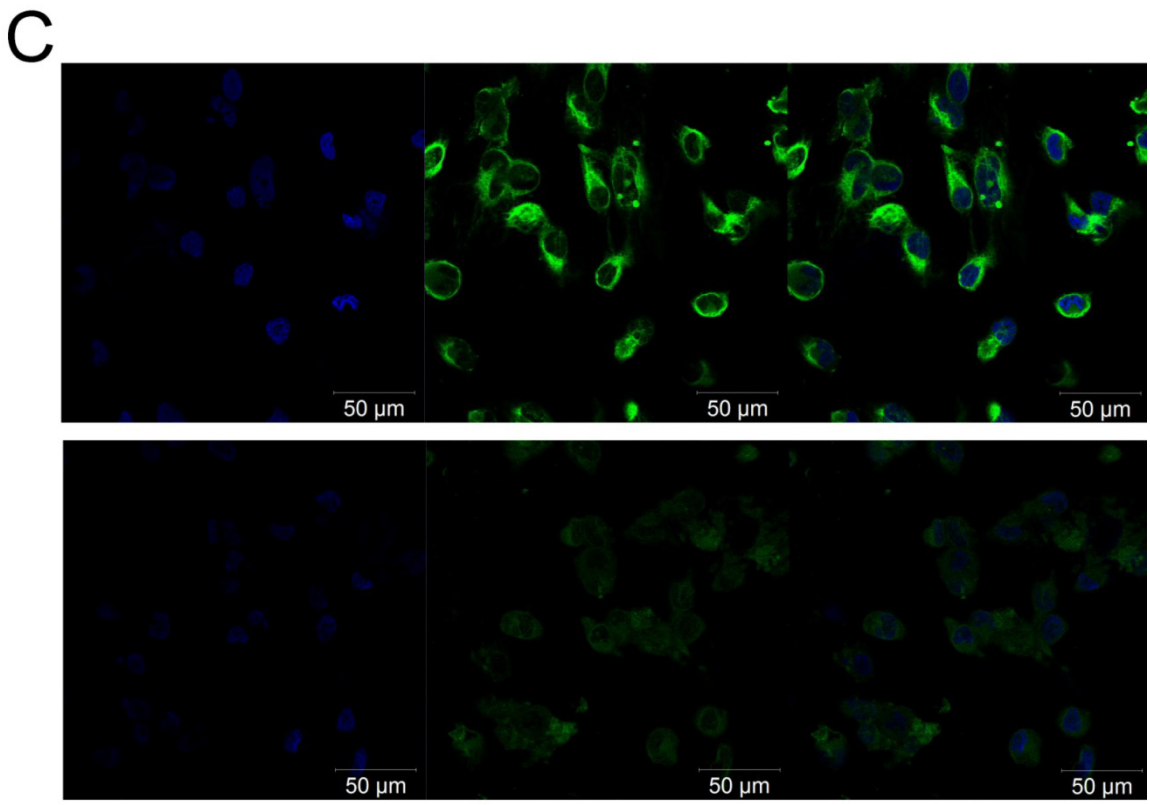

Figure 20: Fluorescent staining images showing the expression of the mesenchymal cytoplasmatic marker Vimentin in hFOB cells after 3 days of culture on A) cp-Ti, B) PEEK and C) Y-TZP disks. Mouse IgG negative control of each specimen is shown in boxes below. Original magnification x200; bar = 50 µm.

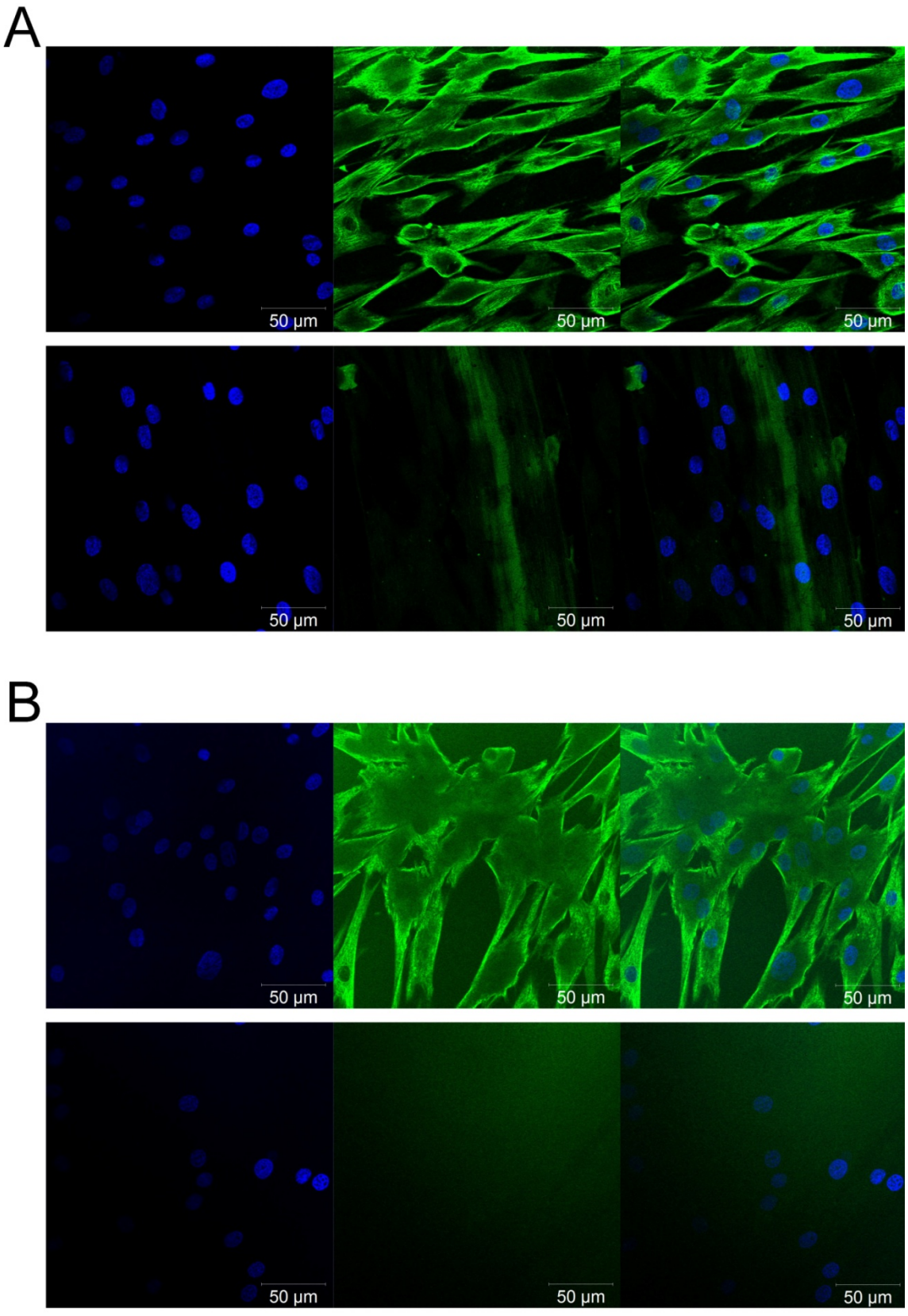
A
50 µm
50 µm
50 µm
50 µm
50 µm
50 µm
B
50 µm
50 µm
50 µm
50 µm
50 µm
50 µm

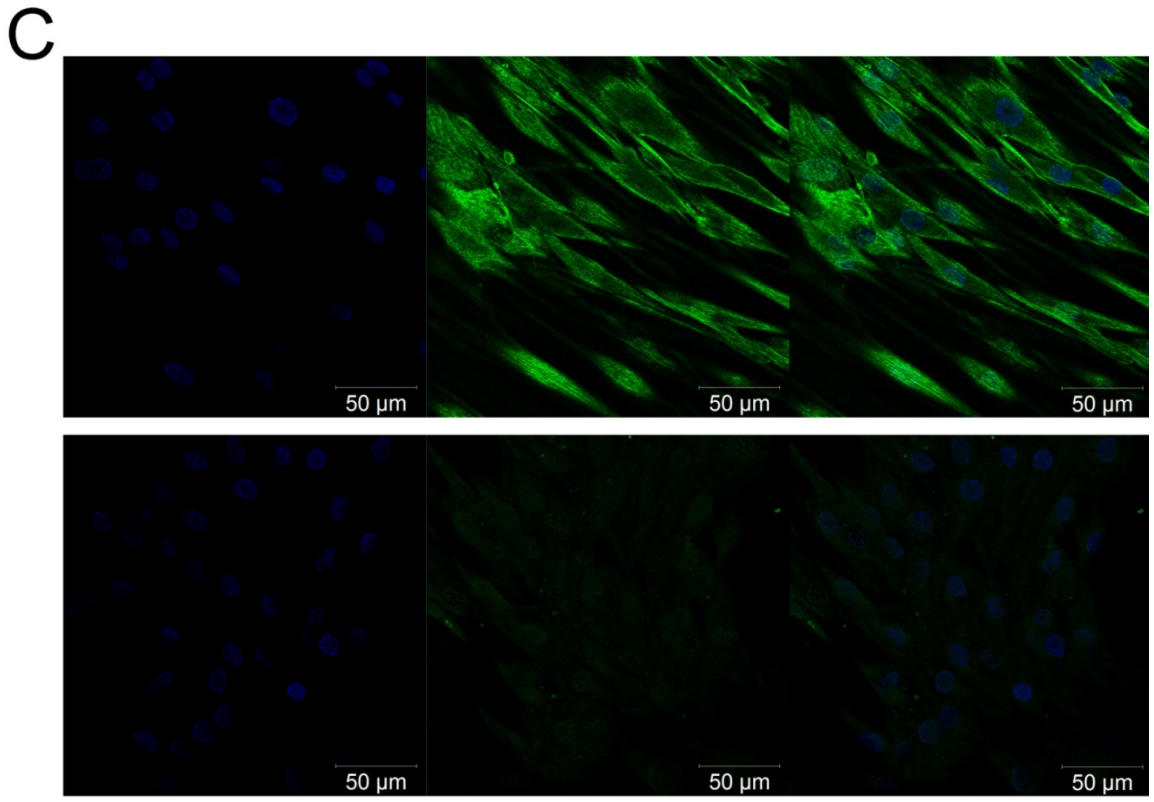

Figure 21: Fluorescent staining images showing the expression of the mesenchymal cytoplasmatic marker Vimentin in hGF cells after 3 days of culture on A) cp-Ti, B) PEEK and C) Y-TZP disks. Mouse IgG negative control of each specimen is shown in boxes below. Original magnification x200; bar = 50 µm.

3.5 Adhesion markers

Cells were tested both genetically and morphologically for expression of the adhesion molecule Vinculin (VCL) through the respective relative gene expression analysis in RT-qPCR and Immunofluorescence staining with Vinculin antibody, both after 3 days in culture, seeded at a cell density of 2.5x 10^4 cells/well.

For RT-qPCR, the polystyrene control group served as the reference value (ratio = 1). Values were mean ± SD of independent experiments performed in triplicates.

In both hFOB (p15, n=5) and hGF (p9, n=6) cell lines, no significant change in VCL expression was registered between the control group and the tested specimens (Fig. 21 A and B).

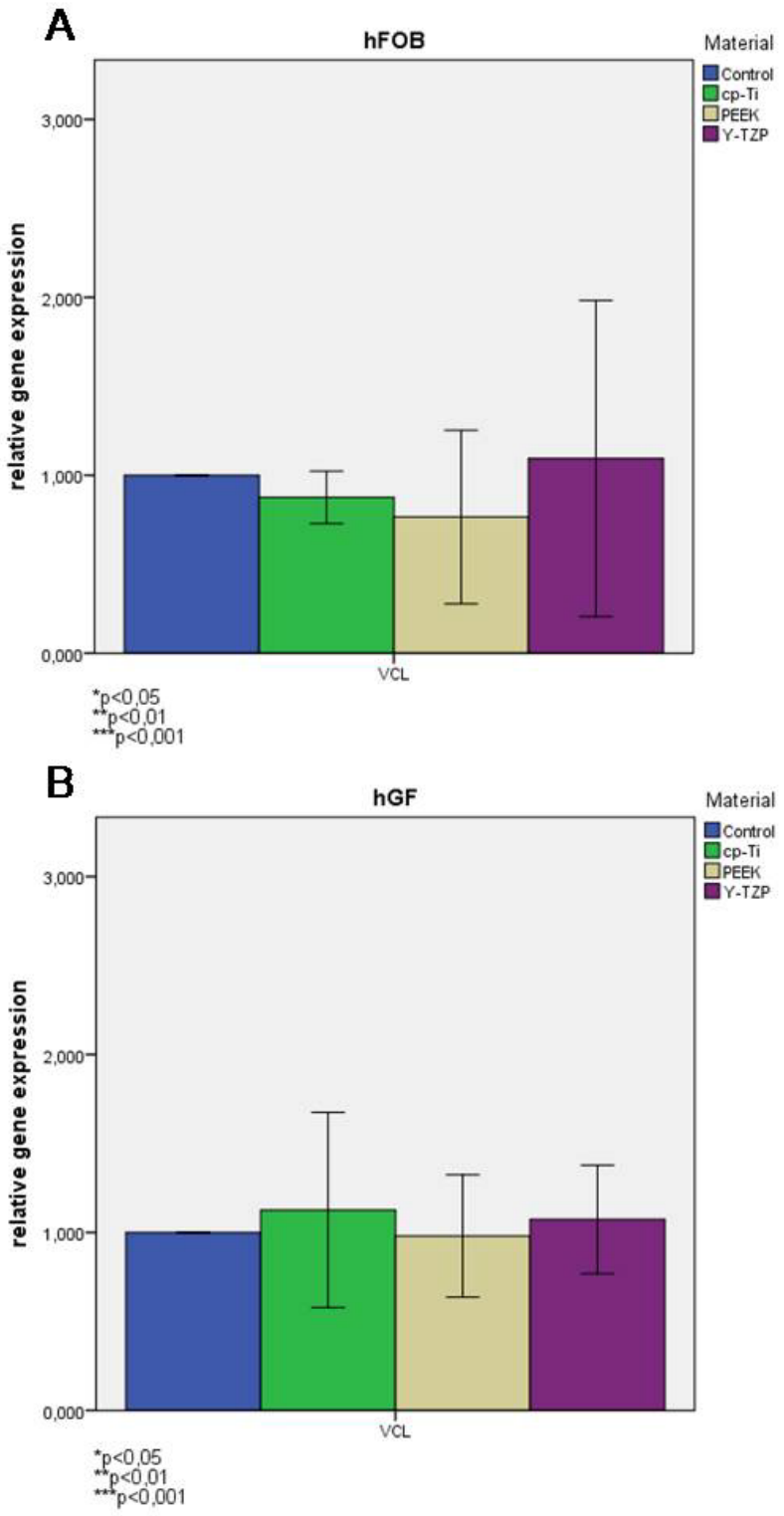

Figure 22: VCL expression was analyzed at mRNA levels in both A) hFOB and B) hGF cells seeded on different dental materials over a period of 3 days. Relative gene expression was measured by RT-qPCR and normalized on reference genes ($2^{-\Delta\Delta Ct}$-method). Data is shown as mean ± SD. Significant p-values are designated in brackets above.

In IF-staining images, cellular morphologies similar to the SEM and Vimentin-staining images in chapter 3.4 can be described.

On control and cp-Ti, hFOB cells showed remarkably higher staining grades of Vinculin, cell density rates and numbers of cytoplasmatic extensions when compared to PEEK and Y-TZP (Fig. 22, A to D).

Additionally, cells cultivated on control, cp-Ti and Y-TZP showed typical morphological characteristics of Vinculin expression: small clusters of oblonged cytoplasmatic structures that are located closely near the cell membrane and directed rectangularly towards the cell-matrix interface, sometimes attached to the surrounding extracellular surface through filiform extensions.

A

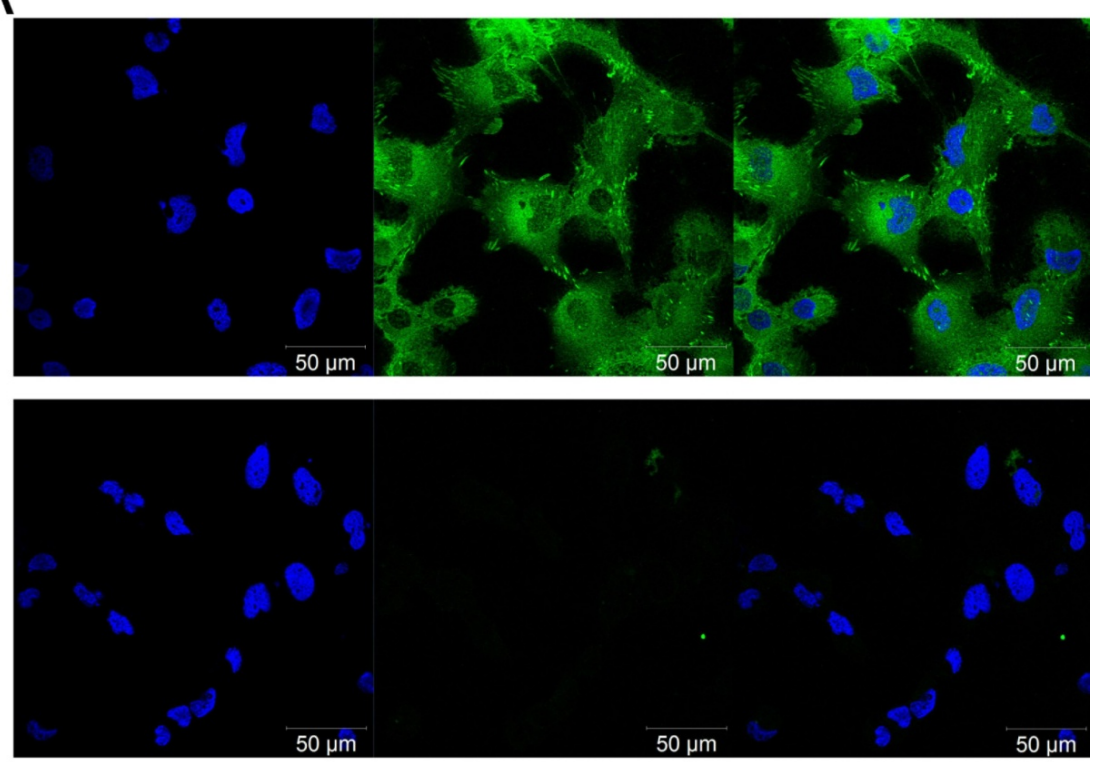

B

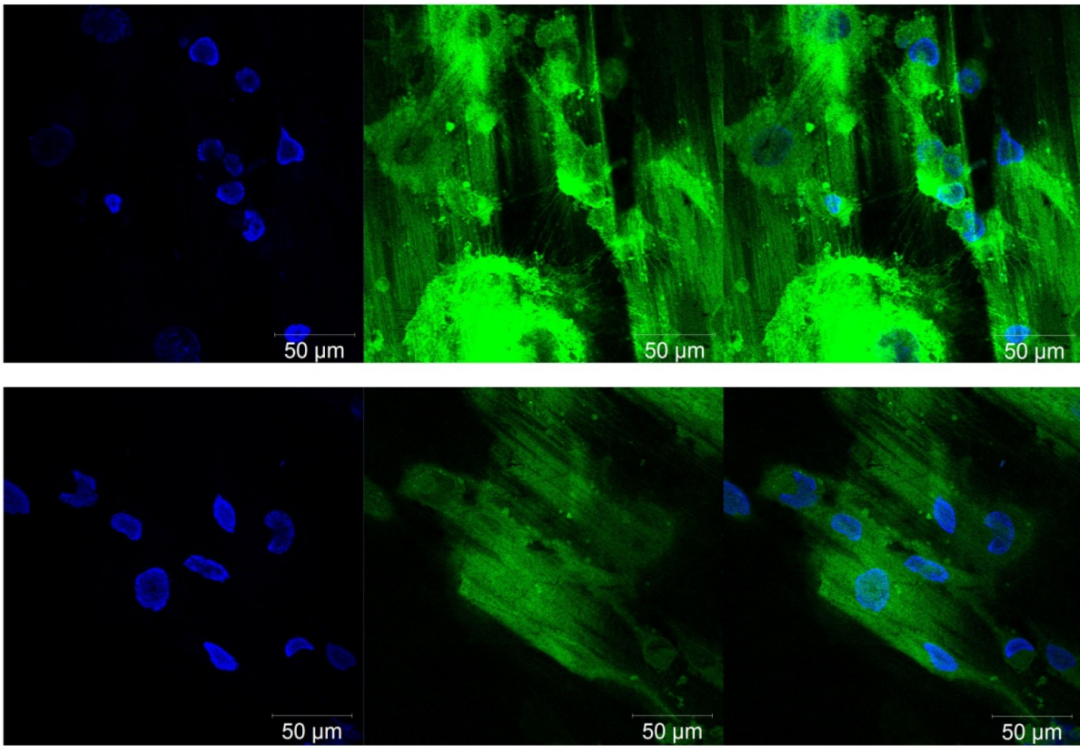

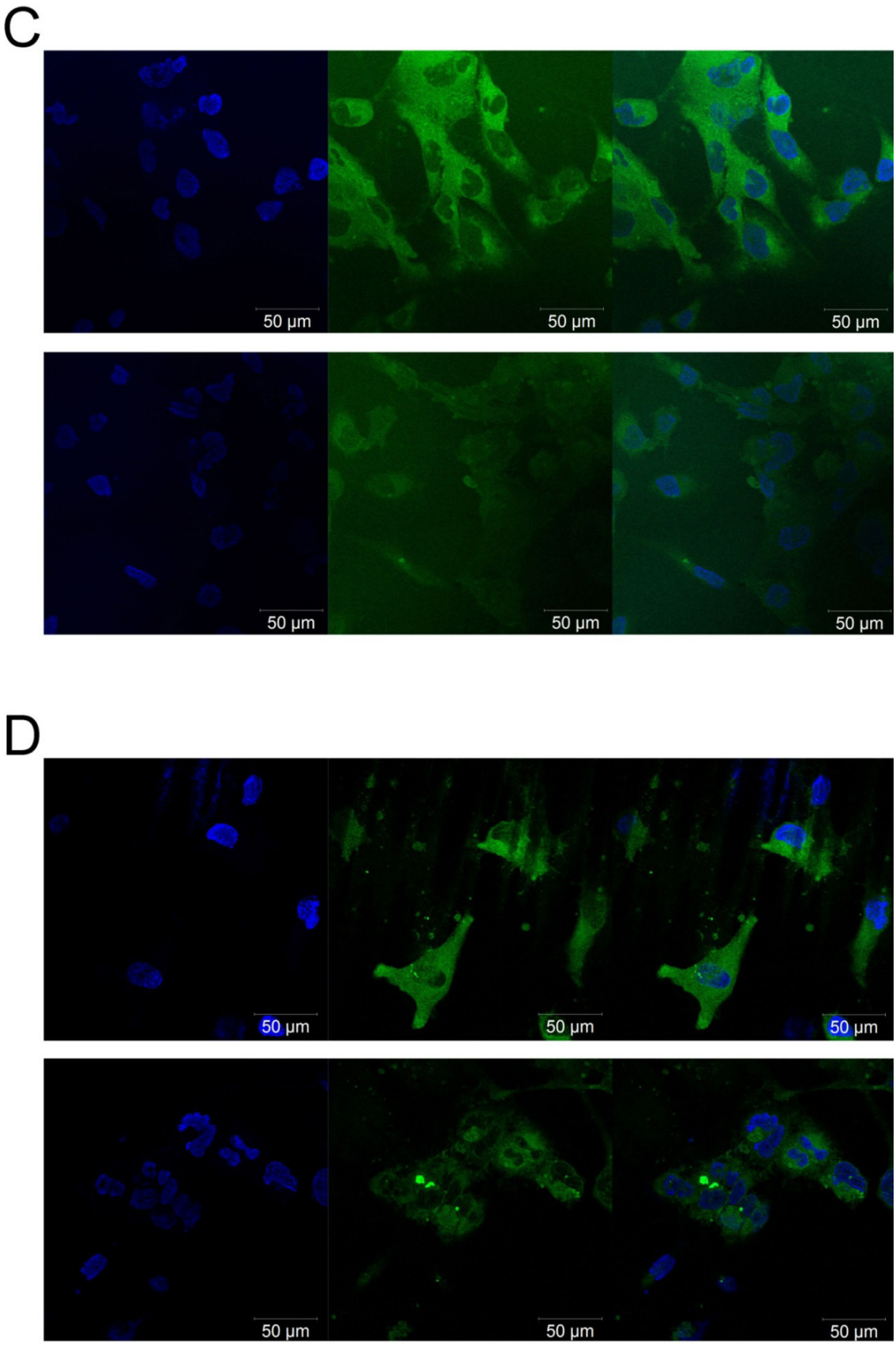

Figure 23: Fluorescent staining images showing the expression of the adhesion marker Vinculin in hFOB cells after 3 days of culture on A) control, B) cp-Ti, C) PEEK and D) Y-TZP. Mouse IgG negative control of each specimen is shown in boxes below. Original magnification x200; bar = 50 µm.

In hGF cells, we observed attachment preferences to the same materials, although this time cells cultivated on Y-TZP showed morphological features equal in quality and quantity to control and cp-Ti (Fig. 23 A to D).
On PEEK, however, they showed a slightly weaker staining and no clear signs of the typical Vinculin expression patterns mentioned above when compared to the other groups (Fig. 23 B).
Again, auto-fluorescence was high in cp-Ti and PEEK specimens in both cell lines.

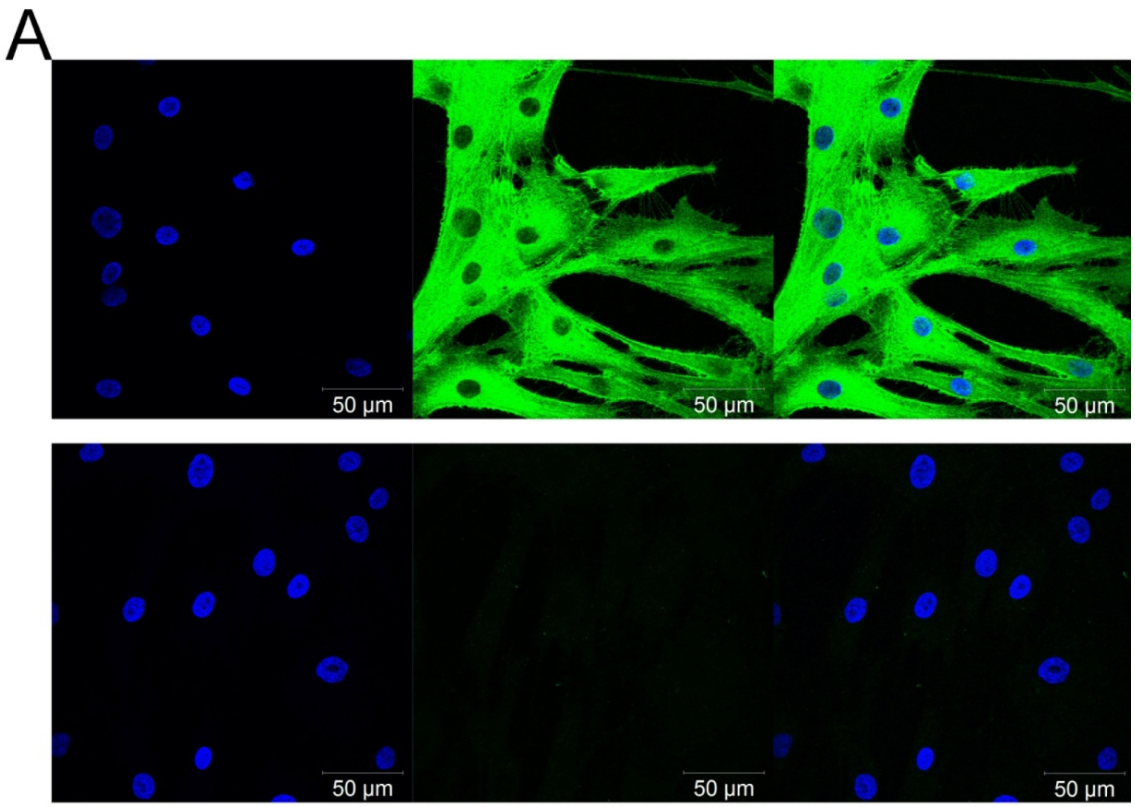
A
50 µm
50 µm
50 µm
50 µm
50 µm
50 µm

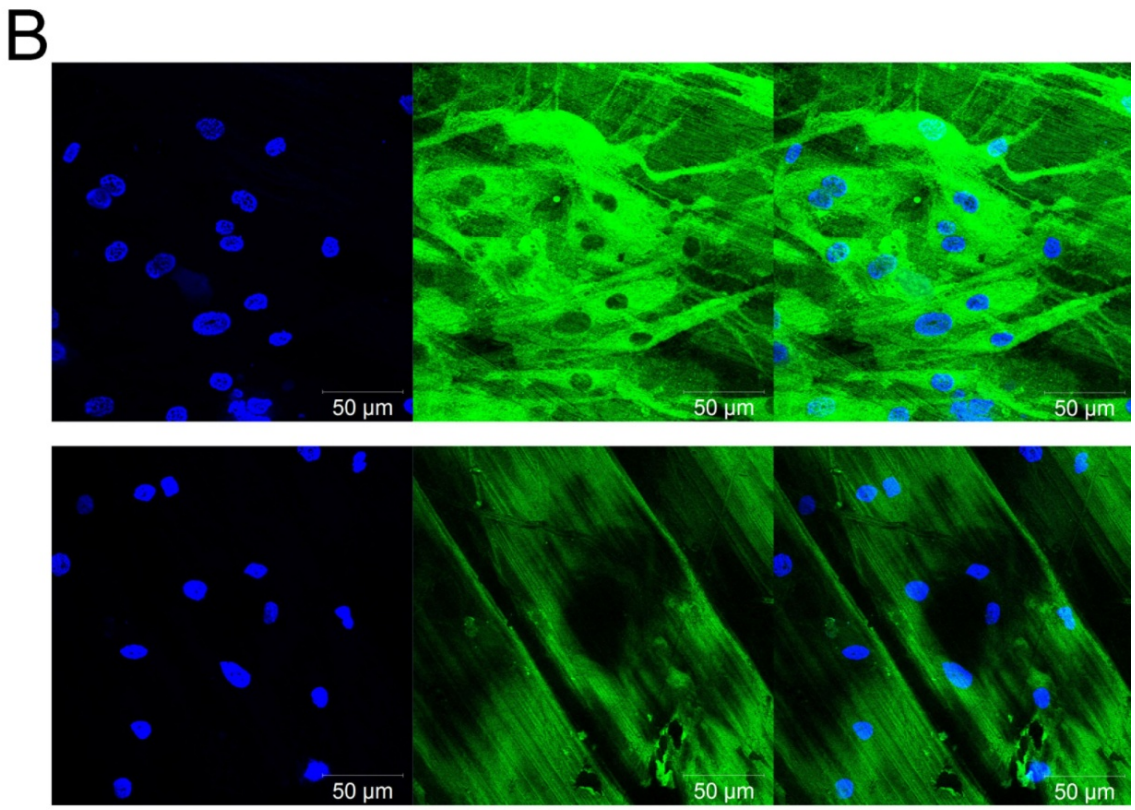
B
50 µm
50 µm
50 µm
50 µm
50 µm
50 µm

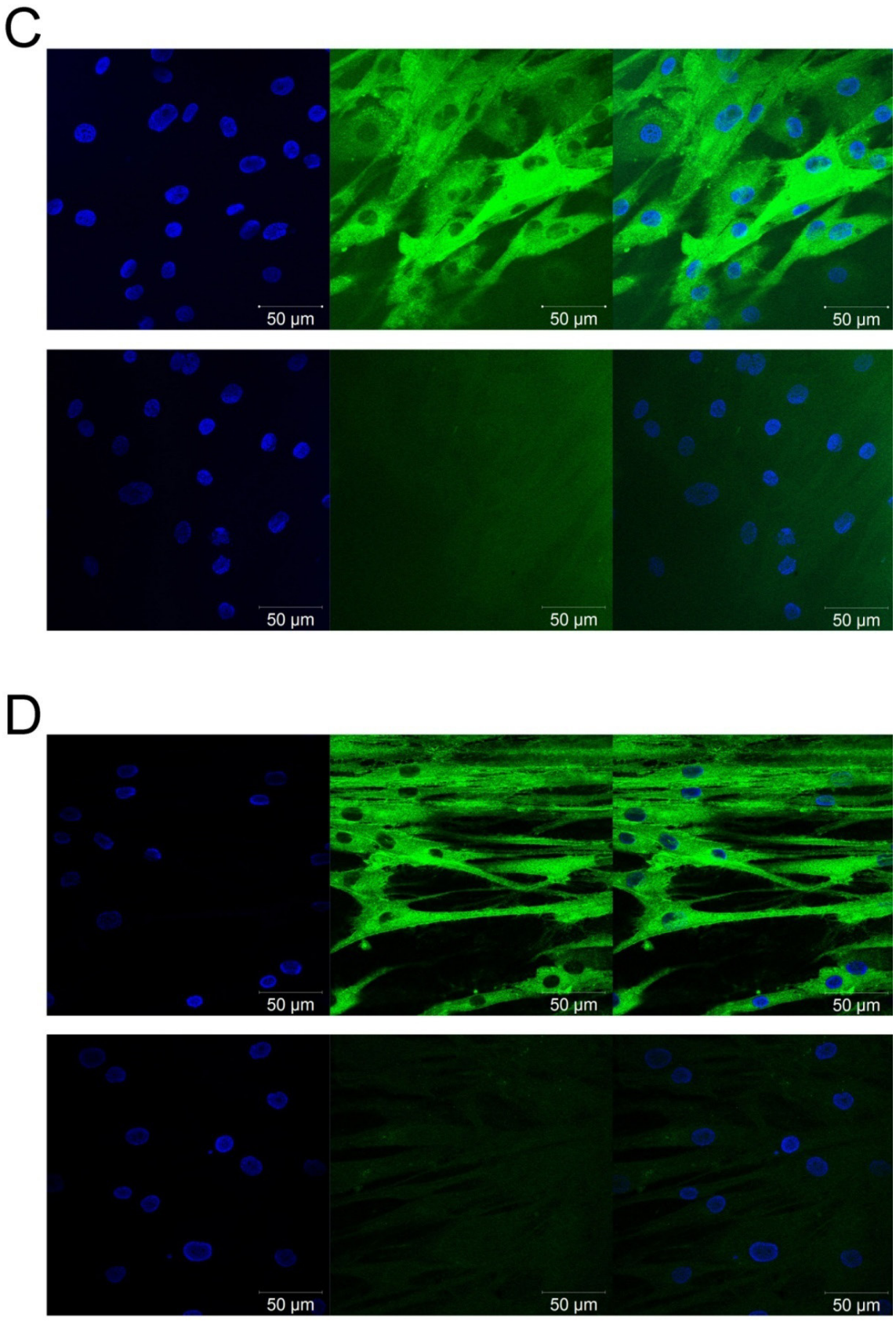

Figure 24: **Fluorescent staining images showing the expression of the adhesion marker Vinculin in hGF cells after 3 days of culture on A) control, B) cp-Ti, C) PEEK and D) Y-TZP. Mouse IgG negative control of each specimen is shown in boxes below. Original magnification x200; bar = 50 µm.**

4 Discussion

“So this other guy, he's a Terminator like you, right?”
“Not like me. T-1000, advanced prototype. Made of mimetic polyalloy.”
“What the hell does that mean?”
“*Liquid metal.”*
(John Connor and The Terminator in “Terminator 2: Judgment Day“) (40)

Technical developments in dental implants have resulted in success rates similar to those of tooth-retained dentures (41).
Tissue integration of an implant is directly depending on cellular adhesion and positive interaction of both hard and soft tissue cells with the implant’s surface. Surface characteristics play a fundamental role in conducting cellular attachment, migration and proliferation of osteoblasts and fibroblasts, two central cell types involved with the process of osseointegration in the alveolar bone (42).
Establishment of a bone-to-implant interface in the initial phase is very important for the prevention of infection and crucial for the success of immediate-loaded implants. (43)
Osteoblasts responsible for the deposition of calcified matrix play a major role in secondary stabilization of the implant while fibroblasts can intervene with the process through excessive formation of soft tissue in the peri-implant region, reducing long-term stability of the implant.
Therefore, osteoblast attachment should be maximized and fibroblast attachment and proliferation should be minimized on the implant’s surface.

In a dental suprastructure exposed to the microbiological flora of the oral cavity however, attachment of any kind of organism can lead to accumulation of a biofilm (an organized compound of synergistic microbiological organisms) and consecutive inflammation of the peri-restorative soft and hard tissue. This process is called periodontitis in the natural tooth or peri-implantitis in a dental implant. If untreated, inflammation of the peri-restorative tissue most certainly leads to a loss of bone attachment and, in the worst case, to the loss of a tooth or the implant. Additionally, health and stability of the peri-implant mucosa at the transitional level (between implant, abutment and suprastructure) also affect the esthetics of the implant (44).

If the purpose of a material is to be applied in the transitional zone or in a dental suprastructure such as a single crown, bridge or a whole denture, cellular attachment should be suppressed to avoid the above mentioned complications. This effect is usually achieved by polishing the material's surface to maximize its grade of smoothness.
Recently however, the importance of the so-called soft-tissue seal, a peri-implant fibrous tissue formation covering the transitional zone is being discussed in maintaining peri-implant health through protecting the underlying osseointegrated implant surface and connective bone layer from inflammatory agents of the oral cavity. In essence, the soft tissue seal in implants is exerting a function similar to the biological width in a natural tooth (45).
Therefore, a surface that is specifically permitting fibroblast attachment while suppressing microbiological adhesion would be preferred for this application.

In this study, we compared the cell proliferation and adhesion behavior of human osteoblasts and gingival fibroblasts on three different materials and surfaces: commercially pure titanium (cp-Ti), yttria-stabilized zirconia (Y-TZP) and filled poly-ether-ether-ketone (PEEK), provided by a commercial retailer of dental implant and restorative suprastructure materials.

We demonstrated that both osteoblasts and fibroblasts cultivated on cp-Ti and Y-TZP showed similar results in all experiments when compared to their respective growth on standardized cell culture plates.
With respect to these findings, we consider both materials to perform equally in proliferation, cytotoxic potential and cellular adhesion. Both materials did not exert any significant differences in all three qualities, demonstrating their biocompatibility for dental applications. The results confirm findings in similar experiments described in the literature. Bächle et al. compared cp-Ti SLA surfaces and standardized polystyrene culture plates to Y-TZP disks with defined surface treatment and R_a-values ranging from 0.15µm to 1µm. There was only a slight reduction after 12 days of culture on machined Y-TZP (R_a ~ 0.15µm) in adhesion of osteoblast-like osteosarcoma cells CAL-72 when compared to the other groups from what could be determined from the proliferation assay and SEM analysis (46). Bergemann et al. confirmed these findings in primary human osteoblast cultures, with empathizing the change in cytoskeletal structures (shortening of

actin filaments) on microroughened Y-TZP surfaces and again demonstrating that machined Y-TZP with low Ra-values (Ra ~ 0.59µm) provides inferior adhesion qualities (47).
Pae et al. yielded equal results for proliferation and SEM adhesion analysis in primary hGF cells on both “smooth” cp-Ti and Y-TZP surfaces with or without micro-grooves of 100µm, with no R_a-values being disclosed in this study. They suggested, however, that Y-TZP abutments with microgrooves may improve the biological/soft tissue seal formation. (48)

In PEEK specimens however, viability measured in the MTS assay was reduced significantly in both cell types when compared to the other groups, while surprisingly the amount of LDH release remained equal.
In both the SEM images and IF staining for Vinculin, hFOB cells cultured on PEEK were less numbered, not evenly spread, exhibited a more cuboidal shape, sharp cell borders and few filopodia with only limited amount of underlying extracellular matrix, suggesting that these cells are predominantly stuck in stage 1 of the 4 stages of cellular attachment defined by Rajaraman et al. in their 1975 publication on cellular adhesion (43). If cells are able to attach to a surface properly, filopodia will be replaced by lamellopodia and the cells will change their shape to polygonal (stage 4). Both lamellopodia and a polygonal shape were observed on control, cp-Ti and Y-TZP surfaces. These findings correlate with topography experiments conducted by Anselme et al., Sammons et al. and Kunzler et al. in which mean surface roughness values (R_a) below 1µm showed significant reduction in cell adhesion and less shape transformation (43,47,48).
In hGF cells, exhibition of lamellopodia and transformation from cubiodal to polygonal cell shape was found on all surfaces, albeit slightly weaker when cultured on PEEK specimens.
Low MTS values and stable cytotoxicity might also be explained through the circumstance of low cellular adhesion on the highly smooth PEEK surface resulting in cells that remain in a metabolically inactive state, processing neither the MTS reagent nor producing relevant amounts of LDH.

Remarkably, LDH release values in all specimens (including control) increased in hFOB cells over time and decreased in hGF cells. We conclude that these findings are related to the diverging doubling time of these two cell types, with fibroblast culture reaching confluence earlier in the observation period of 7 days and subsequently reducing its correlating metabolic activity and LDH release.

4.1 Conclusion

Commercially pure titanium remains the standard material for dental implants.

In SEM observation, both hFOB and hGF cells spread more intimately on machined cp-Ti and Y-TZP surfaces than on a highly polished PEEK surface, with both cell types exhibiting more deposition of extracellular matrix and filamentous extensions, indicating progressive cellular adhesion. Parameters of viability and cytoxicity as well as complementary qPCR expression values and IF staining confirmed these findings.

Data on cp-Ti and Y-TZP surface modification procedures and profilometry parameters was not available from the manufacturer. A direct comparison of surface roughness values would have been desirable to give more clear comments on changes of cellular morphology in this experiment.

In addition, high auto-fluorescence in IF-staining on PEEK made it very difficult to distinguish the sharpness of cell borders in both cell types.

4.2 Implications for the field

Concluding from our findings, filled PEEK with a highly polished surface can be considered inferior to cp-Ti and Y-TZP regarding short-term cellular adhesion of osteoblasts and, from a biological standpoint, might not be considered a reliable material for osseointegrated dental Implant application in the observed state.

Still, PEEK remains a promising compound material due to its highly customable production process, positive functional and esthetic physico-chemical properties, and a low potential of cytotoxicity (as demonstrated before and confirmed in our experiments).

Successful efforts have already been made to improve mechanical and biological stability of PEEK through adding various fillers like titanium or ceramic particles and carbon or glass fibers of defined sizes and lengths (28,49). As a downturn, too

much filler material of gray color can diminish the esthetic advantage of PEEK (as seen on Fig. 5).
Also, no study to date has compared PEEK to the standard material titanium in terms of defined surface roughness values accepted for facilitating osseointegration.
Further modifications and investigations will be necessary to establish PEEK as an implant dentistry material on both the experimental and clinical level.

If decreased adhesion of both cells and microorganisms is desired in applications such as restorative dental suprastructures, polished PEEK seems to be a reasonable choice.
In our experiments, fibroblast growth on PEEK did not increasingly differ from the other specimens. In fact, it has been stated before that adhesion and proliferation of fibroblasts is higher on smooth surfaces and that osteoblasts prefer roughened surfaces (42).Highly polished PEEK could therefore be considered an interesting alternative to commonly available abutment materials in terms of promoting fibroblast proliferation and consecutive soft tissue seal formation while retaining tooth-like biomechanical and esthetic qualities.

4.3 Future experiments

Mechanical forces such as osmotic pressure, tensional forces, prestress, and shear stress are all contributing factors to cellular attachment, proliferation, differentiation, and consecutive tissue development (50).
In accordance with these general facts, it has been shown that surface roughness is a major factor to cellular adhesion in experimental implant biomaterial research (43,51). Other factors such as surface chemistry, surface energy and surface patterns could also play a significant (although minor) role in promoting attachment and proliferation (52).
On the biological level, our study has shown that under static conditions, both cell types were able to exhibit phenotypes and growth patterns similar to standardized cell culture conditions when cultured on the right material and surface. If results are promising or exceeding expectations, experiments in dynamic cell culture (e.g. in a customized bioreactor) or direct implantation in the animal implant model should investigate the impact of the material and its surface on the above

mentioned factors and their role in the sustainable induction of tissue development.
In both static and dynamic culture models, analysis of genetic markers of the osteogenic pathways such as bone morphogenetic protein (BMP)-2 could prove beneficial when measuring osteoinductive qualities. Mesenchymal progenitor and stem cells should be used to appreciate tissue formation from precursor cells.

In material research, experiments including X-ray photoelectron spectroscopy (XPS) could further describe any possible formation of potential cytotoxic compounds after surface finish on PEEK specimens, similar to the experiments conducted by Kang et al. on commercially available titanium implant surfaces (53).
In recent years, it became possible to design and fabricate materials with very precise surface characteristics on the nanoscale level, applying techniques such as nano-stereolithography and a refined version of galvanostatic anodization (54). It became feasible not only to create distinctive patterns such as grooves and lanes of varying orientation, length and width, but also to cover these surfaces with various resorbable and biocompatible coatings of biomimetic substances like calcium phosphate apatite crystals or even bioactive substrates such as the above mentioned bone morphogenetic protein (BMP), proliferative proteins like fibroblast growth factor (FGF) or adhesive peptides like fibronectin (52,55).

5 Literaturverzeichnis / References

1. Cameron J. The Terminator. Orion Pictures; 1984.

2. Bionics - MeSH - NCBI [Internet]. [cited 2016 Jan 31]. Available from: http://www.ncbi.nlm.nih.gov/mesh/?term=bionics

3. Thurston AJ. Paré and Prosthetics: The early history of artificial limbs. ANZ J Surg. 2007 Dec;77(12):1114–9.

4. Alt KW. Die historische Entwicklung der zahnärztlichen Prothetik. In: Strub JR, Kern M, Türp JC, Witkowski S, Heydecke G, Wolfart S, editors. Geschichte, Grundlagen, Behandlungskonzept, Vorbehandlung (Curriculum Prothetik). 4th ed. Berlin: Quintessenz-Verl; 2011. p. 1-15.

5. Oscar Pistorius makes Olympic history in 400m at London 2012 - BBC Sport [Internet]. [cited 2016 Jan 31]. Available from: http://www.bbc.com/sport/olympics/18911479

6. Schimmel M, Katsoulis J, Genton L, Müller F. Masticatory function and nutrition in old age. Swiss Dent J. 2015;125(4):449–54.

7. Williams DF. On the nature of biomaterials. Biomaterials. 2009 Oct;30(30):5897–909.

8. Williams DF. On the mechanisms of biocompatibility. Biomaterials. 2008 Jul;29(20):2941–53.

9. Bergmann CP, Stumpf A. Biomaterials. In: Dental Ceramics [Internet]. Berlin, Heidelberg: Springer Berlin Heidelberg; 2013 [cited 2016 Jan 31]. p. 9–13. Available from: http://link.springer.com/10.1007/978-3-642-38224-6_2

10. Restorations with CEREC | Sirona Dental [Internet]. [cited 2016 Feb 7]. Available from: http://www.sirona.com/en/products/digital-dentistry/restorations-with-cerec/

11. Branemark P-I. Osseointegration and its experimental background. J Prosthet Dent. 1983 Sep;50(3):399–410.

12. Albrektsson T, Brånemark PI, Hansson HA, Lindström J. Osseointegrated titanium implants. Requirements for ensuring a long-lasting, direct bone-to-implant anchorage in man. Acta Orthop Scand. 1981;52(2):155–70.

13. Rosa MB, Albrektsson T, Francischone CE, Schwartz Filho HO, Wennerberg A. The influence of surface treatment on the implant roughness pattern. J Appl Oral Sci Rev FOB. 2012 Oct;20(5):550–5.

14. Wennerberg A, Albrektsson T. On implant surfaces: a review of current knowledge and opinions. Int J Oral Maxillofac Implants. 2010 Feb;25(1):63–74.

15. Elias CN, Lima JHC, Valiev R, Meyers MA. Biomedical applications of titanium and its alloys. JOM. 2008;60(3):46–9.

16. ASTM International. Specification for Titanium and Titanium Alloy Castings [Internet]. Available from: http://dx.doi.org/10.1520/b0367

17. Freese HL, Volas MG, Wood JR. Metallurgy and Technological Properties of Titanium and Titanium Alloys. In: Titanium in Medicine [Internet]. Berlin, Heidelberg: Springer Berlin Heidelberg; 2001 [cited 2016 Feb 7]. p. 25–51. Available from: http://link.springer.com/10.1007/978-3-642-56486-4_3

18. Sicilia A, Cuesta S, Coma G, Arregui I, Guisasola C, Ruiz E, et al. Titanium allergy in dental implant patients: a clinical study on 1500 consecutive patients. Clin Oral Implants Res. 2008 Aug;19(8):823–35.

19. Mu Y, Kobayashi T, Sumita M, Yamamoto A, Hanawa T. Metal ion release from titanium with active oxygen species generated by rat macrophages in vitro. J Biomed Mater Res. 2000 Feb;49(2):238–43.

20. Mellinghoff J. Zehn Jahre Implantologie mit Keramikimplantaten - Einsichten und Aussichten. Zahntech Mag. 2014 May;18(5):264–8.

21. Andreiotelli M, Kohal R-J. Fracture strength of zirconia implants after artificial aging. Clin Implant Dent Relat Res. 2009 Jun;11(2):158–66.

22. Chevalier J, Gremillard L, Deville S. Low-Temperature Degradation of Zirconia and Implications for Biomedical Implants. Annu Rev Mater Res. 2007 Aug;37(1):1–32.

23. Özkurt Z, Kazazoğlu E. Zirconia Dental Implants: A Literature Review. J Oral Implantol. 2011 Jun;37(3):367–76.

24. Bona A, Pecho O, Alessandretti R. Zirconia as a Dental Biomaterial. Materials. 2015 Aug 4;8(8):4978–91.

25. Andreiotelli M, Wenz HJ, Kohal R-J. Are ceramic implants a viable alternative to titanium implants? A systematic literature review. Clin Oral Implants Res. 2009 Sep;20 Suppl 4:32–47.

26. Payer M, Heschl A, Koller M, Arnetzl G, Lorenzoni M, Jakse N. All-ceramic restoration of zirconia two-piece implants--a randomized controlled clinical trial. Clin Oral Implants Res. 2015 Apr;26(4):371–6.

27. Kurtz SM, Devine JN. PEEK biomaterials in trauma, orthopedic, and spinal implants. Biomaterials. 2007 Nov;28(32):4845–69.

28. Schwitalla A, Müller W-D. PEEK dental implants: a review of the literature. J Oral Implantol. 2013 Dec;39(6):743–9.

29. Schwitalla AD, Abou-Emara M, Spintig T, Lackmann J, Müller WD. Finite element analysis of the biomechanical effects of PEEK dental implants on the peri-implant bone. J Biomech. 2015 Jan 2;48(1):1–7.

30. Lee W-T, Koak J-Y, Lim Y-J, Kim S-K, Kwon H-B, Kim M-J. Stress shielding and fatigue limits of poly-ether-ether-ketone dental implants. J Biomed Mater Res B Appl Biomater. 2012 May;100(4):1044–52.

31. Kallage I. Bewertung des Belastungs- und Verformungsverhaltens ausgewählter PEEK-Compounds für zahnärztliche Anwendungen [Internet]. [Berlin]: Freie Universität Berlin; 2015 [cited 2016 Feb 21]. Available from: http://www.diss.fu-berlin.de/diss/servlets/MCRFileNodeServlet/FUDISS_derivate_000000016401/Diss_Ilona_Kallage.pdf

32. U.S. Department of Health and Human Services. Use of International Standard ISO- 10993, "Biological Evaluation of Medical Devices Part 1: Evaluation and Testing." 2013 Apr 23;1–38.

33. Schroeder HE. Orale Strukturbiologie: Entwicklungsgeschichte, Struktur und Funktion normaler Hart- und Weichgewebe der Mundhöhle und des Kiefergelenks. 5., unveränd. Aufl. Stuttgart: Thieme; 2000. 421 p.

34. Promega Corporation. CellTiter 96® AQueous One Solution Cell Proliferation Assay Technical Bulletin TB245 [Internet]. 2012 [cited 2016 Mar 6]. Available from: https://at.promega.com/~/media/files/resources/protocols/technical%20bulletins/0/celltiter%2096%20aqueous%20one%20solution%20cell%20proliferation%20assay%20system%20protocol.pdf

35. Promega Corporation. CytoTox-ONE™ Homogeneous Membrane Integrity Assay Technical Bulletin TB306 [Internet]. 2009 [cited 2016 Mar 6]. Available from: https://at.promega.com/~/media/files/resources/protocols/technical%20bulletins/101/cytotox-one%20homogeneous%20membrane%20integrity%20assay%20protocol.pdf

36. Jpark623. overview of rt-pcr technique. In: Wikipedia, the free encyclopedia [Internet]. 2015 [cited 2016 Mar 6]. Available from: https://en.wikipedia.org/w/index.php?title=Reverse_transcription_polymerase_chain_reaction&oldid=688041684

37. Bustin SA, Benes V, Garson JA, Hellemans J, Huggett J, Kubista M, et al. The MIQE Guidelines: Minimum Information for Publication of Quantitative Real-Time PCR Experiments. Clin Chem. 2009 Apr 1;55(4):611–22.

38. Bohn W, Wiegers W, Beuttenmüller M, Traub P. Species-specific recognition patterns of monoclonal antibodies directed against vimentin. Exp Cell Res. 1992 Jul;201(1):1–7.

39. Asijee GM, Sturk A, Bruin T, Wilkinson JM, Ten Cate JW. Vinculin is a permanent component of the membrane skeleton and is incorporated into the (re)organising cytoskeleton upon platelet activation. Eur J Biochem FEBS. 1990 Apr 20;189(1):131–6.

40. Cameron J. Terminator 2: Judgment Day. TriStar Pictures; 1991.

41. Le M, Papia E, Larsson C. The clinical success of tooth- and implant-supported zirconia-based fixed dental prostheses. A systematic review. J Oral Rehabil. 2015 Jun;42(6):467–80.

42. Anselme K, Bigerelle M. Role of materials surface topography on mammalian cell response. Int Mater Rev. 2011 Jul;56(4):243–66.

43. Sammons RL, Lumbikanonda N, Gross M, Cantzler P. Comparison of osteoblast spreading on microstructured dental implant surfaces and cell behaviour in an explant model of osseointegration: A scanning electron microscopic study. Clin Oral Implants Res. 2005 Dec;16(6):657–66.

44. Atsuta I, Ayukawa Y, Kondo R, Oshiro W, Matsuura Y, Furuhashi A, et al. Soft tissue sealing around dental implants based on histological interpretation. J Prosthodont Res. 2016 Jan;60(1):3–11.

45. Dhir S. Peri-Implant and Periodontal Tissues: A Review of Differences and Similarities. Compend Contin Educ Dent. 2013 Aug;34(7).

46. Bächle M, Butz F, Hübner U, Bakalinis E, Kohal RJ. Behavior of CAL72 osteoblast-like cells cultured on zirconia ceramics with different surface topographies. Clin Oral Implants Res. 2007 Feb;18(1):53–9.

47. Bergemann C, Duske K, Nebe JB, Schöne A, Bulnheim U, Seitz H, et al. Microstructured zirconia surfaces modulate osteogenic marker genes in human primary osteoblasts. J Mater Sci Mater Med [Internet]. 2015 Jan [cited 2016 Jan 10];26(1). Available from: http://link.springer.com/10.1007/s10856-014-5350-x

48. Pae A, Lee H, Kim H-S, Kwon Y-D, Woo Y-H. Attachment and growth behaviour of human gingival fibroblasts on titanium and zirconia ceramic surfaces. Biomed Mater. 2009 Apr;4(2):25005.

49. Jung H-D, Park H-S, Kang M-H, Li Y, Kim H-E, Koh Y-H, et al. Reinforcement of polyetheretherketone polymer with titanium for improved mechanical properties and in vitro biocompatibility. J Biomed Mater Res B Appl Biomater. 2016 Jan;104(1):141–8.

50. Mammoto T, Ingber DE. Mechanical control of tissue and organ development. Development. 2010 May 1;137(9):1407–20.

51. Bigerelle M, Anselme K, Noël B, Ruderman I, Hardouin P, Iost A. Improvement in the morphology of Ti-based surfaces: a new process to increase in vitro human osteoblast response. Biomaterials. 2002 Apr;23(7):1563–77.

52. Duraccio D, Mussano F, Faga MG. Biomaterials for dental implants: current and future trends. J Mater Sci. 2015 Jul;50(14):4779–812.

53. Kang B-S, Sul Y-T, Oh S-J, Lee H-J, Albrektsson T. XPS, AES and SEM analysis of recent dental implants. Acta Biomater. 2009 Jul;5(6):2222–9.

54. McNamara LE, McMurray RJ, Biggs MJP, Kantawong F, Oreffo ROC, Dalby MJ. Nanotopographical control of stem cell differentiation. J Tissue Eng. 2010;2010:120623.

55. Kulkarni M, Mazare A, Gongadze E, Perutkova š, Kralj-Iglič V, Milošev I, et al. Titanium nanostructures for biomedical applications. Nanotechnology. 2015 Feb 13;26(6):62002.